THE SYNTHESIS AND CHARACTERIZATION OF CHEMICAL SENSORS AND THEIR APPLICATION TO ANIONS AND HEAVY METAL IONS SENSING

A MINI THESIS SUBMITTED IN PARTIAL FULLFILMENT

OF THE REQUIREMENTS FOR THE DEGREE OF

MASTER OF SCIENCE (CHEMISTRY)

OF

THE UNIVERSITY OF NAMIBIA

BY

MARTHA NIISHIYE AMPUTU

200613154

APRIL 2022

MAIN SUPERVISOR: Prof. Veikko Uahengo (University of Namibia)

ABSTRACT

Cations and anions play a major role in the biological and physiological processes in living organisms attracting more research interest in the area of chemical sensing. However, the excessive accumulation of ions in living organisms, particularly in humans, is toxic and can lead to health problems. Chemosensing is a powerful tool that can be employed to detect these ions in an environment. This is due to their high selectivity and sensitivity for the target analytes. Therefore, this research worked on designing two dual receptors namely **A** and **C.** These chemosensors were designed based on the fluorophore-spacer-receptor principle and they have been synthesized based on the environmentally friendly and cost-effective Schiff base method. The synthesized chemosensors were characterized using a Proton Nuclear Magnetic Resonance (^{1}H NMR), Fluorescence and Ultraviolet-visible (UV-Vis) spectrophotometer.

The research findings have indicated that both receptor **A** and receptor **C** are colorimetrically and spectroscopically selective and sensitive to multiple cations and anions. Receptor **A** displayed a naked eye colorimetric sensitivity and spectrally towards; Co^{2+}, Cu^{2+}, Fe^{2+} while with the anions only spectral sensitivity was displayed. For both cations and anions a red shift in absorption with isosbestic points at 286 nm and 284 nm respectively, and fluorescence enhancement were observed, except for Fe^{2+}, were no isosbestic point was observed and fluorescence quenching was noted. Similarly, receptor **C** presented both naked eye colorimetric sensitivity and spectrally towards these anions: CN^{-}, F^{-}, AcO^{-}, OCN^{-}, OH^{-} and these cations: Cu^{2+}, Fe^{2+} Zn^{2+}, Ni^{2+}, Hg^{2+}. A bathochromic shift and fluorescence enhancement were observed with the anions, while for the cations absorption varies depending on the cations' identity. Moreover, fluorescence quenching

was observed with most cations, with an exemption for Hg^{2+} and Al^{3+} with fluorescence enhancement.

Keywords: Chemosensor, naked eye detection, cation, anion, multi-sensing, UV-Vis spectrophotometer, Florescence spectrophotometer, ^{1}H NMR

ACKNOWLEDGEMENTS

Firstly, I would like to thank the Almighty God for his guidance and for granting me the strength to carry out this research and giving me courage to overcome all obstacles I have encountered. Secondly, I would like to thank my supervisor, Prof. Veikko Uahengo, for introducing me to the Chemosensor research and for allowing me to be part of his research group. I would also like to thank him for his supervision and motivation during this study. Special thanks go to Peter Shanika for assisting me with the NMR analysis. I am also indebted to the DAAD for partly sponsoring this research project. Finally, I would like to thank my family for their moral support. All your prayers, help and support are highly appreciated.

DEDICATIONS

To my son Tangeni, my late mother Regina Ndangi Gajus and my dad Ephraim Amputu.

DECLARATIONS

I, Martha N. Amputu, hereby declare that this study is my own work and is a true reflection of my research, and that this work, or any part thereof has not been submitted for a degree at any other institution.

Martha N. Amputu …… ….……

Name of Student Signature Date

TABLE OF CONTENTS

LIST OF SCHEMES

LIST OF FIGURES

LIST OF ABBREVIATIONS AND/OR ACRONYMS

δ	Chemical shift
π	pi
Abs.	Absorbance
A	Acceptor
$CDCL_3$	Dueterated chroform
CH_3CN	Acetonitrile
DMSO	Dimethyl sulfoxide
D	Donor
d	doublet
ddd	Doublet of doublet of doublets
EtOH	Ethanol
ED	Electron withdrawing
EW	Electron donating
equiv.	Equivalent
H_2O	Water
^1H NMR	Proton Nuclear Magnetic Resonance
ICT	Intramolecular charge transfer
J	Coupling constant

µl	Micro liter
ml	Mililiter
µM	Micro molar
mmol	Milimolar
m	Multiplet
MHz	Mega Hertz
M	Molar
nm	Nano meter
PET	Photoinduced electron transfer
rtp	Room temperature and pressure
s	Singlet
TBA	Tetra butylammonium
UV	Ultra violet
Vis.	Visible
v/v	volume over volume ratio

Chapter 1 Introduction

1.1 Background of the study

The demand for fast and efficient chemical sensing has experienced tremendous growth over the past few years especially in the fields of medical diagnostics, environmental monitoring, and toxicology analysis. Chemical sensors achieve this goal by responding to external stimulus and converting it into a signal which can be measured. According to Czarnick, F. Goppelsrodor was the first to report on fluorescent chemosensor in 1867, where it was used as a method for aluminium ion determination [1]. Chemosensors used to detect other metal ions were further developed, however they could not detect anions at the time. The advancement of fluorescent chemosensor in the early eighties, caused the application to extend to various cations and anions that are essential in biological systems [2].

Moreover, the broader aim of this study is to contribute to a better understanding of developing cheap and environmentally friendly dual multi-sensing colorimetric sensors that are soluble in aqueous environment. This also, in effect, contribute to the response to environmental pollution resulting from industrialization and mining activities that has become a threat, causing contamination in water sources, the air we breathe, and agricultural areas.

1.1.1 The importance of detecting anions and heavy metals ions

The selective detection of ions is extremely essential because of the various roles they have in biological and physiological processes. Anions have noble applications in metabolic process, disease treatment in biological systems [3,4] and others are extremely detrimental [5]. Transitional metals have important applications in biological systems, environment and in industries. In biological systems, heavy metal ions play a role in the catalytic, structural components and regulatory facet [6–8]. Besides the great application of heavy metal ions, others are very toxic. Among them is mercury which is a global pollutant that is very hazardous to both the environment and human health [9]. Therefore, developing selective and sensitive methods for detecting anions and heavy metal ions is very important, in order to understand their environmental benefits and risks.

1.1.2 The nature Schiff bases

Schiff bases, first discovered by the German scientist Hugo Schiff in 1864, are generally represented by the formula $R_1CH=NR_2$ (where R_1 and R_2 are alkyl, aryl, cyclo alkyl or heterocyclic groups) (Scheme1).They are a condensation product of primary amines and carbonyl compounds [10]. In addition, Schiff bases form ligands with strong coordinative ability [11] and have a range of application in various areas such as biological activities, catalysts, pigments and dyes, polymer stabilizers, and corrosion inhibitors [12].

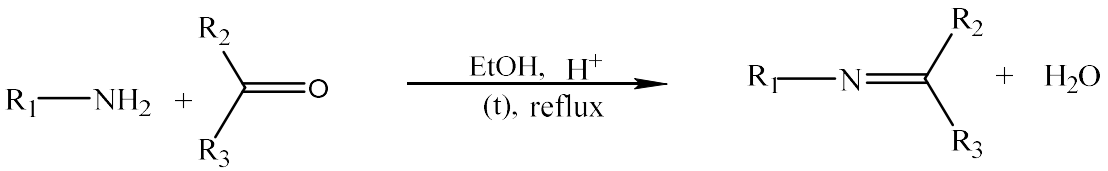

Scheme 1. Schiff base reaction

Various Schiff base ligands have been used in potentiometric sensors as cation carrier for different cations, owed to their active properties they pose such as highly selective, great sensitivity, stability and simplicity. In addition, they allow for direct on-line monitoring; hence, there is no need for sample pre-treatment with sophisticated analytical instruments [13–18].

1.2 Statement of the problem

Toxic heavy metals and anions are increasingly posing a threat to the environment due to technological advancement and expanding economies. Therefore, there is a need to develop low cost, ease-to-apply and real time chemical assays that are uniquely selective and sensitive to toxic ions, in order to compliment the expensive traditional analytical methods. A number of single-ion-sensing sensors for heavy metal and anions have been reported. However, dual/multi-ion-sensing sensors are very limited in literature [19].

1.3 Objectives of the study

The objectives of the study are:

a) To synthesize and characterize chemical sensors.

b) To identify sensors that are sensitive and selective to any of these specific cations of significant interest (Cu^{2+}, Zn^{2+}, Co^{2+}, Fe^{2+}, Ni^{2+} and Hg^{2+}) and anions (F^-, AcO^-, OCN^-, OH^- and CN^-) in the water soluble solvent/mediums.

1.4 Significance of the study

This research focused on developing cheaper real time sensors that are easily synthesized and applicable in any institution involved in environmental monitoring and mineral exploration. Furthermore, the study also focused on synthesizing a multi-sensing sensor. The designing of multi-ions sensors remains a challenge as only a few multi-ion sensors are reported in the literature [19]. The study further contributes to the existing literature with regard to detecting biologically important cations such as copper and zinc in different media systems, especially the physiological system.

1.5 Limitation of the study

Analytical instruments such as ^{1}H NMR that are critical in analyzing the sensors and the sensor-analyte interaction are not available at the University of Namibia. However, arrangements were made for analysis with ^{1}H NMR to be conducted at the University of Cape Town. This caused a delay in obtaining the results on time.

1.6 Delimitation of the study

The scope of the project is limited to the synthesis and characterization of the sensors as well as the identification and quantification of the analytes. The development of sensors into kits based on colorimetric activities will be outside the scope of this project.

Chapter 2. Literature review

Ions play a vital role in the environmental, biological, physiological, and chemical processes. In biological systems, ions are very important in cell generation, oxygen transportation in the blood, treatment of diseases, and plant growth amongst others [3,4,6,20]. Equally, physiological systems ions have vital roles of gene regulation and immune function [6,21], whereas in chemical processes, they are used in mineral extraction, metal fabrication and other applications such as electronics [5,22]. However, when ions are in excess, they are very toxic to the biological system and the environment. It is for this reason that the sensing of anions and heavy metal ions are of great interest to researchers. Negative electrostatic charge is the most prominent characteristic that distinguish anions from other guest species in chemosensing [23].

This review of literature work mainly focused on previous studies that entailed testing chemosensors against the analytes, in order to identify the multi-element sensing chemosensors which is the focal point of this research.

2.1 Chemosensors

In recent years, research has focused on developing simple cost-effective and reliable ways of detecting biologically important ions as well as metal ions and anions that pose a threat to the environment. Evidently, literature depicts that prior research developed chemical sensors that are intensely changing the chemical analysis approach [24]. Chemosensor is defined as “a device that can transform chemical information, ranging from the concentration of a specific sample component to total analysis into an analytically useful signal” [25]. The chemosensor uses the transduction methods such as

optical absorption, luminescence and so forth, in order to recognise and quantify the analyte [26]. The sensor consist of two parts, namely the signalling unit or transducer mechanism for communication and receptor or binding unit that recognise the analyte of interest, usually a choromophore or fluorophore as illustrated in Scheme 2 below [27]. On top of that, the mechanisms used in ion recognition mimic the natural reaction.

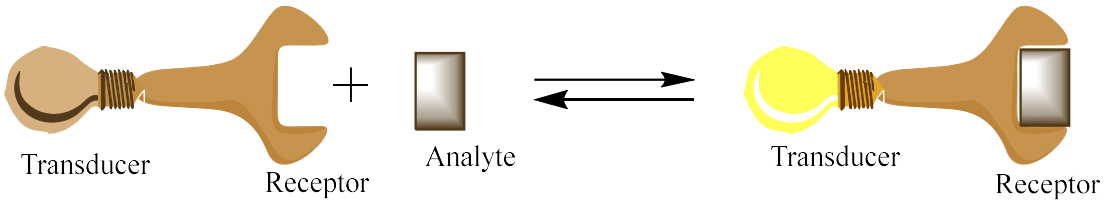

Scheme 2. Operating principle of a chemosensor

According to literature, there are three recognition techniques: binding site signalling subunit approach, displacement approach and chemodosimetric approach [28,29]. Furthermore, the resultant signal sensors are grouped into two categories: optical sensors which result in change in optical properties and electronic sensors which result in change in electrochemical properties [30]. On the other hand, optical sensors are further classified into two categories: the 1) fluorogenic and 2) chromogenic sensors [28].

Chemosensors have numerous applications in various disciplines such as biochemistry, cell biology, environmental monitoring, clinical and medical sciences. In clinical and medical sciences, chemosensors are essential for critical care analyses and are used as markers for diseases [31].

2.1.1 Fluorescent Chemosensors

Fluorescent sensor is defined as a molecular tool capable of signalling the presence of an analyte such as ions or molecule [19,31]. In fluorescence chemosensor, the fluorephore acts as the signal transducer that converts the recognition signal into an optical signal. With fluorescent chemosensor, the nature of the solvent plays a significant role in its ability to recognise and bind the analyte, and it is applicable to both single analyte detection and dual/multi-analyte detection. Additionally, features such as thermal and photochemical stability and reversible recognition process to allow continuous monitoring of the analyte make an ideal fluorescent sensor [1,31]. Moreover, receptor and fluorephore communication are realised by several mechanism such as the π-systems which integrate the electron-donating (ED) and electron–withdrawing (EW) as observed in the internal charge transfer (ICT) or the photoinduced electron transfer (PET). Overall, recognition of ions by fluorescence chemosensors are significantly being favoured due to selectivity, sensitivity, real time response, local response and low detection limit [28,31,32].

2.1.2 Chromogenic Chemosensors

Chromogenic sensors utilize naked eye in analyte detection. They are used as a simple test to determine the presence of an analyte (ion) by colour change [33]. In chromogenic sensors, colorimetry is used as a signal transduction method; whereby two important signal motifs are considered namely: a change in intensity at a certain wavelength and monitoring a change in the maximum absorption [31].

The chromogenic sensors are synthesized based on molecule compounds containing one or more optical signalling chromophic groups, covalently or noncovalently linked to the receptor moiety [34]. They have been utilized for decades due to the ease of detection, cost-effective, simplicity and easy to access. However, chromogenic sensors are less sensitive and have high detection limit, but still in millimolar concentration range than fluorogenic sensors due to the reduced background [31]. Chromogenic sensors have been widely used in diagnostic assays such as early pregnant test, testing presence of drug in urine and blood-glucose monitoring [35,36].

2.2 Anion sensors

Hydrogen bonding groups have been extensively used as binding sites in anion recognition. The receptors with functional groups such as: thiourea/urea, amides pyrrole, phenol, phenylhydrazone and others are used in fluorogenic or chromogenic anion sensing through the hydrogen bonding interactions [37–43]. Hydrogen bonding is the most useful and effective non-covalent interaction in anion sensing [42]. The development of new design strategies with effective binding sites and signalling units for anion detection has been the focal area of research [3,44].

Patra et al. designed and synthesized hydrazone colorimetric chemosensor based on Schiff base. The synthesized compound **1** (Figure 1) was applied in the detection of CN^-. Upon the addition of CN^-, naked-eye visual detection of compound **1** with colour change from yellow to red in acetonitrile and water mixture. The changes were attributed to the deprotonation of the –NH and the -OH proton by CN^-. Furthermore, the sensitivity,

selectivity, binding stereochemistry and binding constant were also determined [45].

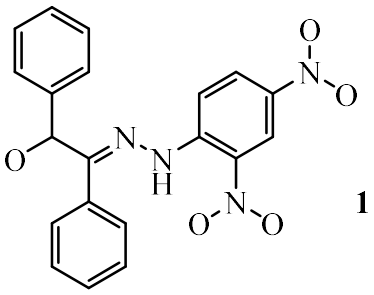

1

Figure 1. Structure of the receptors **1** [45].

2.2.1 The target Anions

2.2.1.1 Acetate ions

Acetate ions play an essential role in the metabolic process and is a key indicator of organic decomposition in marine sediments [3]. Acetate is also used to make industrial chemicals as well as in the manufacturing of paints, textiles, dye, paper and plastics [3,46]. It is also used as a modifier of food starch. Humans and animals are exposed to acetate through inhalation of contaminated air and oral or dermal contact with contaminated water or products containing the acetate compounds. Exposure to high concentration of acetate affects the respiratory system causing irritation of the nose and throat as well as damaging the respiratory tract [46].

Goswami et al. designed and synthesized pterin based sensor **2** (Figure 2) that is highly selective and sensitive to acetate. The synthesized pterin sensor **2** was applied in the detection of acetate in acetonitrile, which resulted in the naked eye detection with a change of colour from light yellow to violet. The change is attributed to the creation of the

hydrogen bonds and deprotonation of the amide proton which influence the electronic properties of the chromophore [47].

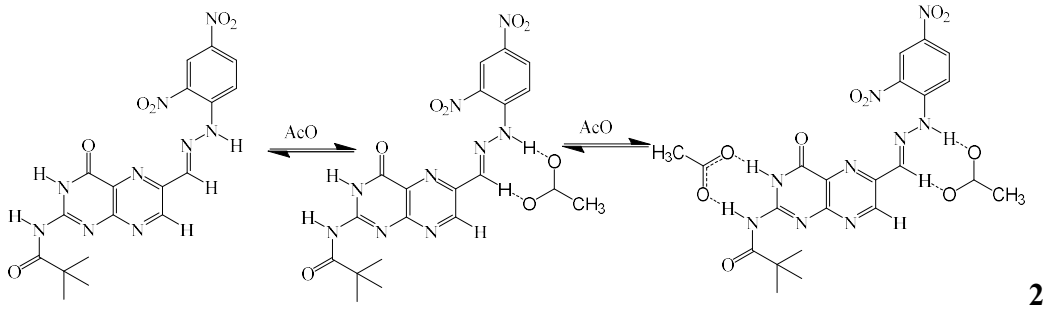

2

Figure 2: Structure of the receptor **2** and the interaction of **2** and acetate [47]

2.2.1.2 Cyanate ions

Cyanate ion in a form of ester resins are used in aerospace and microelectronics due to the unique properties such as low moisture absorption, good adhesion to metals and other substrates and radar transparency [48]. However, other forms of cyanates such as cyanate that is formed from the spontaneous decomposition of urea, known as uremic toxin, is toxic to humans. Cyanate is linked to endothelial dysfunction [49].

2.2.1.3 Cyanide ions

Cyanide ion is one of the anions that is key for gold leaching, petroleum, chemical and metal industries. Additionally, micro-organisms use cyanide as a source of carbon and nitrogen [50]. However, cyanide ion is very detrimental to humans, aquatic life and the environment [5,51]. Cyanide ion affects the nervous systems, metabolism system, cardiovascular system and can lead to death [52,53].

2.2.1.4 Fluoride ions

Fluoride is an essential anion in the human body that plays a fundamental role in the biological functions such as the treatment for osteoporosis and dental caries. In addition, fluoride ion is one of the most targeted anion because of its unique properties such as being the smallest anion and having a strong basicity and high charge density [4,54,55]. However, excess amount of fluoride ion (F^-) is toxic as it can cause diseases such as fluorosis, acute gastric, urolithiasis, bone diseases and cancer [56–59].

A thiourea based multi sensor was synthesized by Kumar et al. that is highly selective to cyanide and fluoride. The thiourea sensor **4** (Figure 3) was applied in the detection of cyanide and fluoride ions in DMSO, which resulted in the naked eye detection. As a result, the colour of sensor **4** changed from pale yellow to red with the addition of cyanide and fluoride ions. This change is attributed to the strong hydrogen bonding with NH [60].

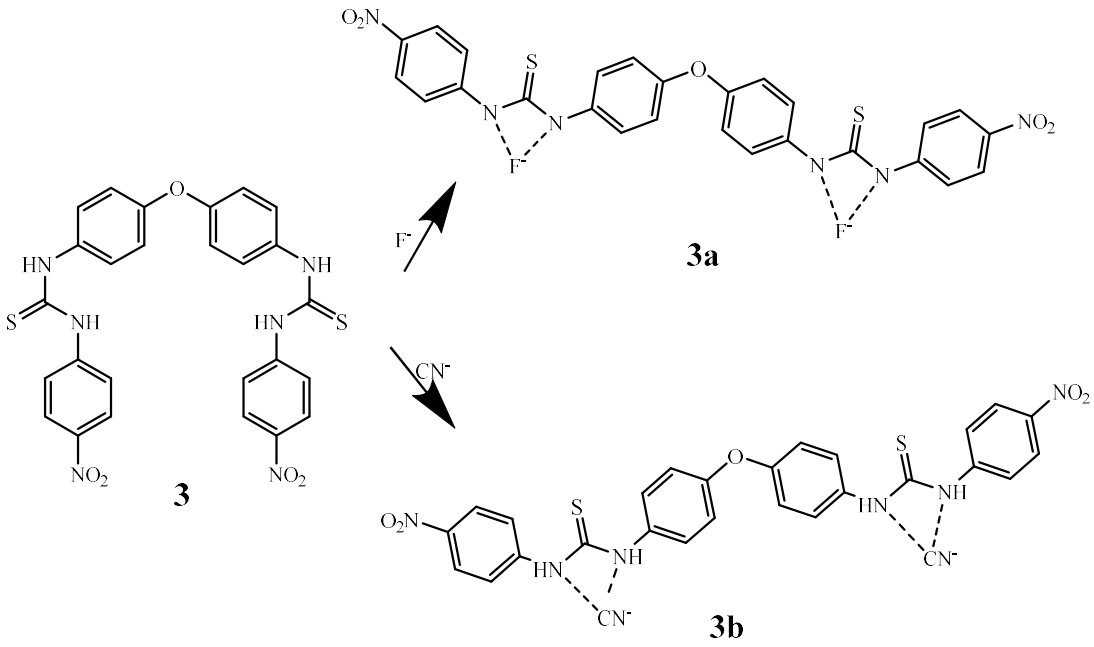

Figure 3: Structure of the receptor **3, 3a** and **3b,** their interaction with respective ions [60].

2.2.1.5 Hydroxides ions

Hydroxide is a compound found in the natural occurring clay minerals. It has many applications where the layered double hydroxides have great properties such as anion exchangeability, composition flexibility and biocompatibility. These properties made the layered double hydroxides to be utilized in drug delivery, water purification, imaging catalysis, separation, biomedicine, energy storage and other environmental application [61–64].

Furthermore, a pyrrole-based Schiff base chemosensor was designed and synthesized by Velmathi et al. for the detection of OH^-. The synthesized sensor **4** (Figure 4) was applied

in the detection of OH^- in CH_3CN, and the colour changed from yellow to purple upon the addition of the OH^-. Additionally, a red shift and fluorescence enhancement were also observed. This is attributed to the complete deprotonation of the amine proton due to the internal charge transfer [65].

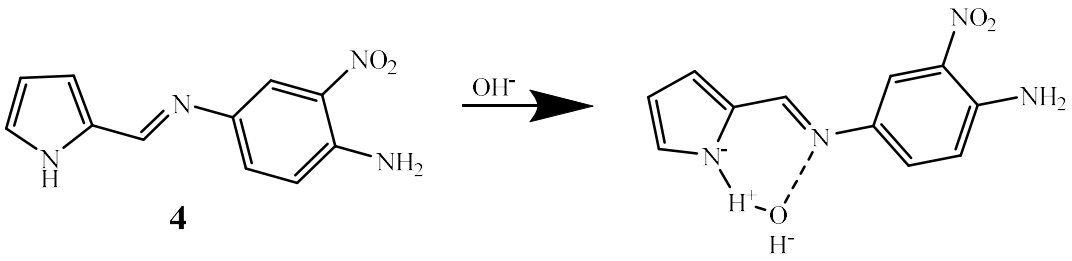

Figure 4: Structure of the receptor **4** and the interaction with hydroxide [65].

2.3 Cation sensors

Cation recognition has been achieved through fluorescent and colorimetric sensors. For colorimetric determination, several moieties such as nitro-phenyls, pyrene, BODIPY, rhodamine, anthracene, fluorescein, and so forth conjugated to an appropriate binding unit mainly through Schiff base, amide linkage and diazo, are applied [29,66]. Rhodamine containing chemosensors and chemosensor with a D-π-A system are the types that are used in colorimetric detection. The latter is achieved by introducing an electron donating (ED) groups and electron withdrawing (EW) groups in the chemosensor at appropriate positions. Furthermore, it is noted that the binding of the metal ion to the chemosensor depends on the hardness and the softness of the binding sites [29]. Despite cation sensors being the first ones to be reported many decades ago, they are still a thrust area in receptor chemistry research [44].

Patra et al. reported on the Schiff base thiourea based chromogenic and flourogenic multiple cation chemosensor. The group designed and synthesized compound **5** (Figure 5) which was successfully applied in the detection of Cu^{2+}, Hg^{2+} and Ag^{+}. The spectra behaviour of the receptor was studied in a methanol-water solution. The reported chemosensor did not only serve as a cation sensor but also as a multiple-cation sensor. The addition of Cu^{2+}, Hg^{2+} and Ag^{+} to compound **6** naked-eye detection was observed with colour change from colourless to deep yellow for Cu^{2+} and to light yellow for Hg^{2+} and Ag^{+}. The chromogenic activity of the sensor **6** is attributed to selective binding of the metals in which the electron density rearranged from donor to acceptor, causing the enhancement of ICT process. Additionally, fluorescence quenching was observed for Hg^{2+} and Ag^{+} while for Cu^{2+} there was a slight band shift with very small intensity [67].

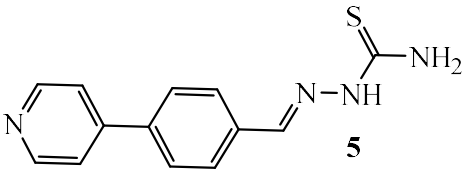

5

Figure 5. Structure of the receptor **5** [67].

2.3.1 The target heavy metals ions

2.3.1.1 Cobalt ions

Cobalt is among the low abundant trace metals found in rocks, soils and fish. Cobalt has chemical properties similar to nickel and iron [68,69]. It plays a vital role in biological systems by being the main component of vitamin B_{12} [6,21,68–70]. On the other hand, it is essential for physiological functions by regulating gene expression, functioning of the immune system and treatment of anaemia [6,21,68]. Cobalt is also used in the increasing

technology such as batteries and electronics [21]. Conversely, excessive exposure to this element is toxic to humans and the environment. The toxicological effects of cobalt in humans include dermatitis respiratory and cardiovascular diseases and the inhalation of cobalt dust has a negative effect on the respiratory system [71,72]. In spite of that, the deficiency of cobalt in human can cause neurologic problems and blood diseases [68].

Liu et al. synthesized a colorimetric and ratiometric chemosensor based on coumarin derivative. Sensor **6,** (Figure 6) was used in the detection of Co^{2+} in acetonitrile-water (1:1, v/v), which resulted in naked eye colour change from yellow to red. Additionally, selective and ratiometric absorbance changes were also detected, with the validation of the selectivity towards cobalt investigated with competitive experiments that could not be detected [72].

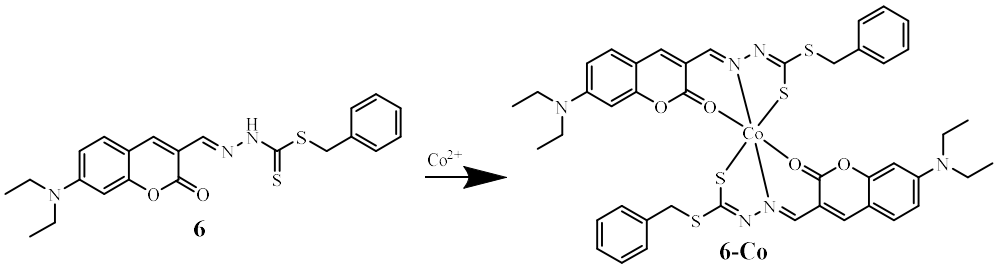

Figure 6. Structure of the receptor **6** and possible binding mode of **6**-Co [72].

2.3.1.2 Copper ions

Copper is the third most abundant transitional metal that is essential in the human body [73,74], physiological and biological processes [6]. It is an essential constituent of enzymes. Contrary, an excess amount of Cu^{2+} is poisonous and can cause Wilson's

disease, dyslexia, hypoglycemia, Alzheimer's disease and various disorders associated with neurodegenerative ailments [7,75–77].

Uahengo et al. reported on the design and synthesis of a fluoro-choromogenic sensor 2, 2′-Dinaphtholazobenzene **7** (Figure 7)**.** This dual sensor was successfully applied in determining Cu^{2+} and F^- simultaneously. Upon the molar addition of Cu^{2+}, the color of sensor **7** changed from red to green; similarly, with the molar addition of F^-, the color changed from red to reddish-brown. Additionally, **7** fluorescent quenching was observed with addition of Cu^{2+} as a result of dissociation of the hydroxyl group. These changes depict the chromogenic and fluorogenic features of **7** [78]**.**

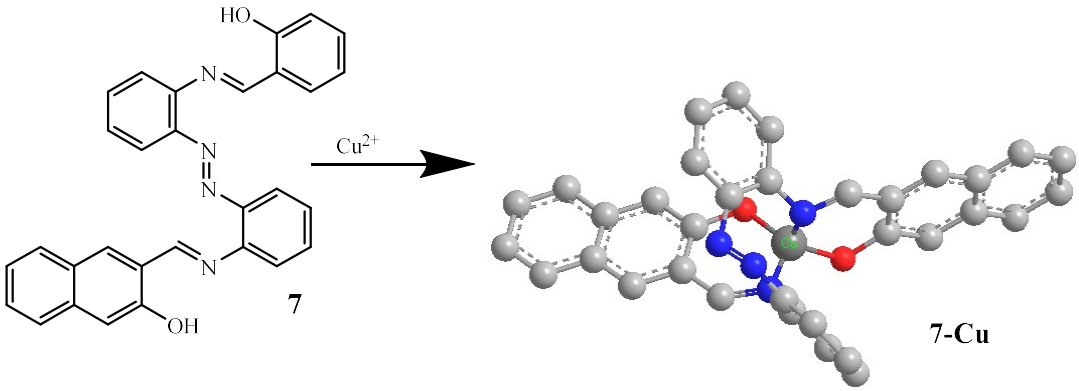

Figure 7. Structure of the receptor **7** and **7**-Cu [78]

2.3.1.3 Iron ions

Iron is the second most abundant metal in the earth's crust [79] and it is first most abundant transitional metal [73]. It can exist in various oxidation states with ferric and ferrous as key players. It is also an essential metal for most living organisms; plants and

microorganisms obtain iron from the environment while humans obtain it through the food chain and supplements [79]. Additionally, iron plays a role as an oxygen carrier in haemoglobin, cellular metabolism and enzyme catalysis [8,20,80]. Though iron plays an important role, its deficiency leads to anaemia [76], increases the risk of perinatal death preterm delivery and low birth weight [81]. On the other hand, excess iron causes neurodegenerative diseases [8].

Rana et al. reported on a colorimetric sensor for detecting iron. The synthesized sensor **8** (Figure 8) was highly selective in detecting Fe^{2+} in an aqueous solvent. Upon the addition of Fe^{2+} to sensor **8,** a red shift was observed associated with colour change from colourless to yellow [82].

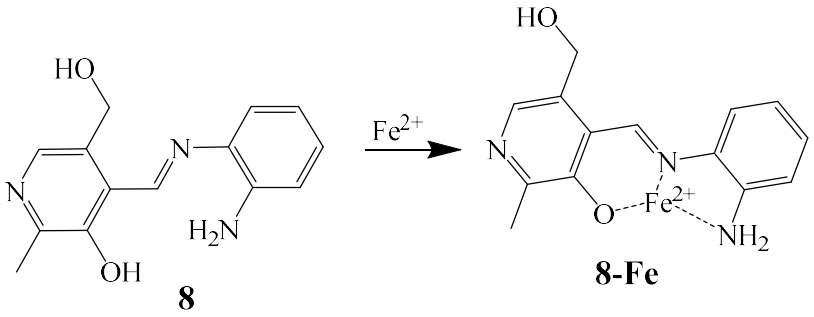

Figure 8. Structure of the receptor **8** and **8**-Fe [82]

2.3.1.4 Mercury ions

Mercury is a naturally occurring transitional metal that exists in three forms, namely elemental, inorganic and organic [83,84]. The organic form of mercury tends to bioaccumulate in the aquatic food chain and then to humans through contaminated fish

consumption [83]. Mercury is widely used in barometers, thermometers, dental amalgam and other industrial uses [85]. However, it is a high mobility element and one of the extremely toxic metals to both humans and the environment. In humans, it can damage the kidneys, brain, central nervous system, reproductive system, respiratory system, and cardiovascular system [85,86].

Jonaghani and Zali-Boeini reported on a fluorescent and colorimetric sensor for detecting Hg^{2+}. The duo synthesized compound **9** (Figure 9) which was highly selective in detecting Hg^{2+} without interference from other metal ions in acetonitrile-water mixture (1:1, v/v). The addition of Hg^{2+} to compound **9** resulted in a colour change from colourless to yellow and a green fluorescent emission [87].

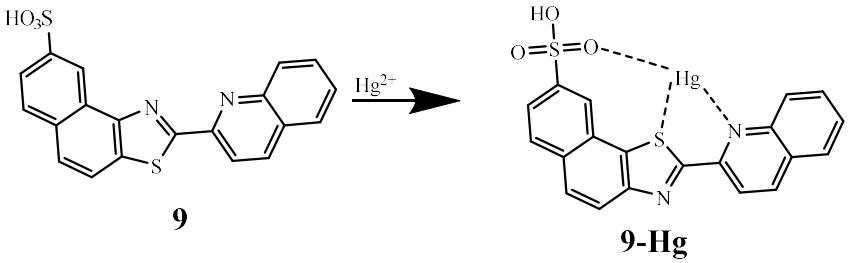

9 **9-Hg**

Figure 9. Structure of the receptor **9** and **9**-Hg [87].

2.3.1.5 Nickel ions

Nickel is a transitional metal and a ferromagnetic element. Nickel plays a vital role in physiological processes and is used in various metallurgical processes [22]. The toxicity of nickel depends on the exposure route and the nickel compound solubility [88].

Prolonged exposure to nickel leads to contact dermatitis, and excess nickel affects the respiratory system [22,88].

Jiang et al. developed a colorimetric sensor based on coumarin derivative. The reported synthesized compound **10** (Figure 10) was successfully applied in the detection of Ni^{2+} in ethanol. Upon the addition of Ni^{2+} to compound **10**, a large red shift was observed, associated with naked eye detection of colour changing from colourless to pink. Additionally, fluorescent quenching of was observed with the addition of Ni^{2+} [89].

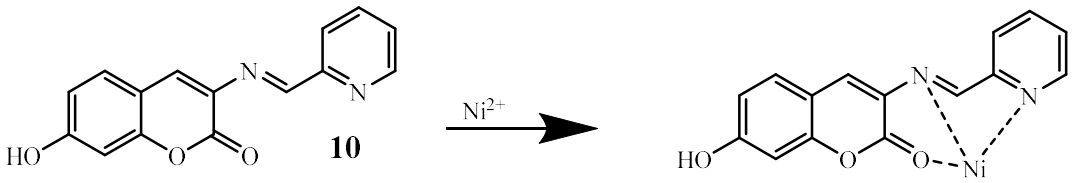

Figure 10. Structure of the receptor **10** and possible binding mode of **10**-Ni [89].

2.3.1.6 Zinc ions

Just like copper, zinc is equally important for physiological and biological processes. Zinc is also the second most abundant transitional metal [73,90]. It is reported that zinc is a cofactor of a number of enzymes that play a crucial role in immune functions such as cell regeneration as well as in catalytic [6,8]. However, zinc deficiency is associated with immune dysfunction, depression and poor wound healing. Similarly, excess zinc in humans is very toxic and it can cause respiratory and gastrointestinal toxicity [79]. Zinc toxicity can also cause sideroblastic anaemia, Alzheimer's disease, Parkinson's disease

and Friedreich's ataxia [6,90]. On the other hand, zinc surplus can lead to excitotoxic neuronal death [8].

An acylhdrazone based fluorescent chemosensor was designed and synthesized by Hu, Li and Sun. The synthesized compound **11** (Figure11) was successfully applied in the detection of zinc in a mixture of H_2O/DMSO (8:2v/v). The addition of zinc to compound **11** resulted in a strong fluorescence response and colour change from colourless yellow-green [91].

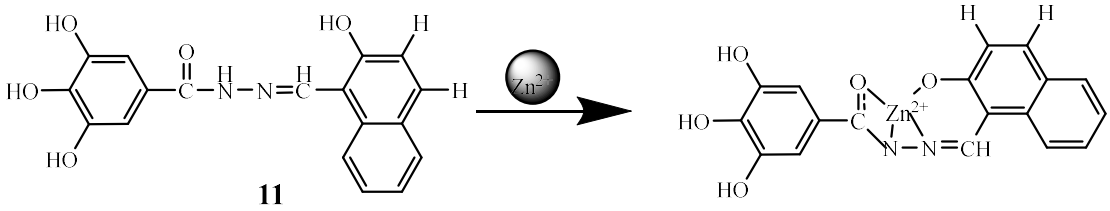

11

Figure 11. Structure of the receptor **11and 11**-Zn [91].

Lastly, from all the sensors reported above for anions and cations, only a few have dual/multi-sensing capabilities. In this study we focused on the synthesis and the characterisation of dual multi sensing chromogenic and fluorescent sensors. We also focused on testing the synthesized sensors against the cations and anions.

Chapter 3: Experimental

3.1 Materials

All chemical reagents used in this study were obtained commercially and are of analytical grade. The chemical reagents were used as received without any further purification. All the anions used are in the form of tetrabutylammonium (TBA) salts. The cations are in either chloride salts or nitrate salts. The chloride salts used are: $FeCl_2 \cdot 4H_2O$, $SnCl_2 \cdot 2H_2O$, $CrCl_3 \cdot 6H_2O$, $MgCl_2$, $MnCl_2 \cdot 4H_2O$, $CuCl_2 \cdot 2H_2O$, $CdCl_2 \cdot H_2O$, $SrCl_2 \cdot 6H_2O$, $AlCl_3$, and the nitrate salts used $Ni(NO_3)_2 \cdot 6H_2O$, $AgNO_3$, $Hg(NO_3)_2 \cdot H_2O$, $Zn(NO_3)_2 \cdot 6H_2O$, $Co(NO_3)_2 \cdot 6H_2O$, $Pb(NO_3)_2$, $Fe(NO_3)_3 \cdot 9H_2O$. Solvents such as dimethyl sulfoxide (DMSO) and ethanol (EtOH) were used. All fluorescence titration and UV-Vis titration were analysed using a ($1x10^{-5}$M) solution of receptor **A** and receptor **C**. The stoichiometric interactions were determined by Job plot using a ($1x10^{-4}$M) solution of receptor **A** and receptor **C** at ambient temperature.

3.2 Instrumentation

UV-Vis spectra were obtained on a Perkin Elmer Lambda 35 UV-Vis spectrophotometer using a 3.0 ml quartz cell with 1cm path length. The fluorescence emission spectra were recorded on a SpectraMax M2 using a quartz cell. The synthesized chemical sensors were characterized using ^{1}H-NMR (400 MHz, DMSO-d_6) analysis at University of Cape Town. All the synthesis and measurements were carried out at ambient temperature.

3.3 Research Methods

3.3.1 Synthesis of the receptors

In this research, we worked on two receptors, namely **A** and **C**. The two receptors are colorimetric and fluorescent dual multi-sensing. The receptor **A** contains two amine and two thiourea groups, whereas receptor **C** bears an amine and a hydroxyl group. The receptor **A** and receptor **C** were synthesized through a simple and one-step Schiff base reaction.

3.3.1.1 Synthesis of receptor A

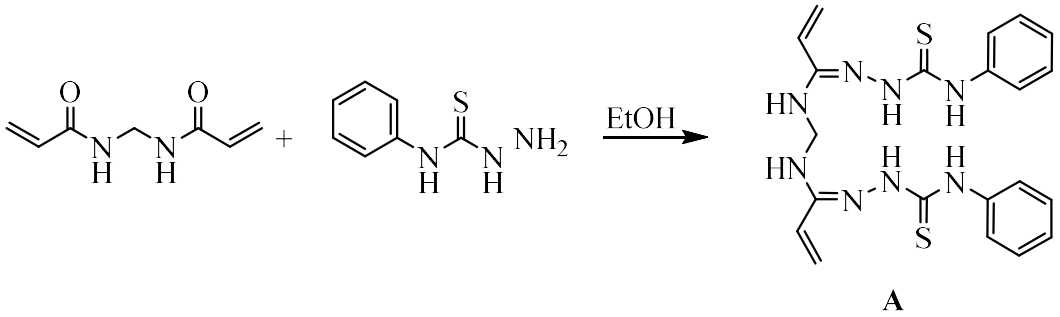

A

Scheme 3. Synthesis route of receptor **A**

The receptor **A** (Scheme 3) was synthesized by dissolving N, N'-methylenebis (acrylamide) (1.0037g 6.49mmol) in 25.0 ml of ethanol. N'phenylhydrazine carbothioamide (2.17 g, 12.98 mmol) was also dissolved in 25.0 ml of ethanol. The two solutions were mixed while magnetically stirred in a round bottom flask with an addition of 3 drops of acetic acid. The mixture was refluxed for 5 hours in a water bath. The solution was filtered and then the crude product was purified by recrystallizing with cold ethanol (100ml) and dried under reduced pressure. Yield: 2.2084 g, 74.9%.

3.3.1.2 Synthesis of receptor C

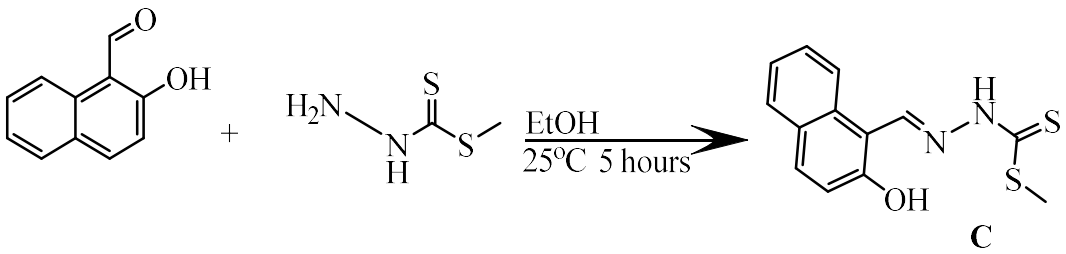

C

Scheme 4. Synthesis route of receptor **C**

A solution of 2-hydroxy-1-naphthaldehyde (1.0019g, 5.81mmol) in 25.0 ml of ethanol was mixed with ethanol solution of 25.0ml of equimolar quantity of hydrazinecarbodithioic acid, methyl ester (0.7116g 5.81mmol) at room temperature in a round bottomed flask. Then, 3 drops of acetic acid were added to the mixture as a catalyst and the mixture was refluxed with vigorous stirring for 5 hours. The crude yellow product was filtered and washed several times with hot ethanol. The product was further dried in vacuum at ambient temperature and recrystallized with hot ethanol, the product (yield 1.2811g, 79.6%). The reaction mechanism of receptor **C** is shown in Scheme 4.

3.3.2 UV-Vis titration measurements

The UV-Vis titrations were performed at ambient temperature. First, 3.0 ml of receptor**s** **A** and **C** (1 x 10^{-5}M) in DMSO were measured separately to determine their absorbance. Subsequently, the interaction of receptor **A** and receptor **C** and the ions were measured separately by molar addition of anions (1 x 10^{-5}M): AcO^-, F^-, CN^- , OH^- , Br^-, Cl^-, ClO_4^-,

HSO_4^-, I^-, N_3^-, NO_3^-, $H_2PO_4^-$ as TBA salts and cations (1 x 10^{-5}M): Cu^{2+}, Fe^{2+}, Ag^+,Al^{3+}, Cd^{2+}, Co^{2+}, Cr^{3+}, Mg^{2+}, Mn^{2+}, Pb^{2+},Ni^{2+}, Sn^{2+},Sr^{2+} and Zn^{2+} with 0.1 equivalent intervals.

3.3.3 Fluorescence titration measurements

The fluorescent intensity of receptor **A** and receptor **C** were measured by withdrawing 3ml of receptor **A** and receptor **C** (1 x 10^{-5}M) in DMSO and their excited states were determined. The fluorescence titrations of receptor **A** and receptor **C** were performed by molar addition at 0.1 equivalent interval of ions (1 x 10^{-5}M): anions AcO^-, F^-, CN^- , OH^- , Br^-, Cl^-, ClO_4^-, HSO_4^-, I^-, N_3^-, NO_3^-, PO_4^{3-} as TBA salts and cations Cu^{2+}, Fe^{2+}, Ag^+,Al^{3+}, Cd^{2+}, Co^{2+}, Cr^{3+}, Mg^{2+}, Mn^{2+}, Pb^{2+},Ni^{2+}, Sn^{2+},Sr^{2+} and Zn^{2+}.

3.3.4 Jobs plot measurements

The stoichiometric interactions of the receptor and ions were measured using Job plots by preparing a series of anion solutions of AcO^-, F^-, CN^-, OH^- (1x10^{-4}M) and cation solutions of Cu^{2+}, Fe^{2+}, Co^{2+}, $Ni^{2+}$and Zn^{2+} (1x10^{-4}M) in DMSO. A standard solution of each receptor **A** and receptor **C** (1x10^{-4}M) was prepared and varying volumes of anions and cations ranging from 0 to 10.0ml (i.e. 1ml guest (F^- or Cu^{2+}) ion and 9.0 ml host (receptor **A** or receptor **C**)) and the absorbance were measured. The process was repeated with all the listed anions and cations with ratios ranging from 1 to 9.

Chapter 4: Results and Discussions

4.1 The interaction of receptor A with different ions

4.1.1 Charaterisation of receptor A

The receptor **A** has been synthesized by Schiff base condensation reaction. The design of the sensor yielded a receptor-spacer-fluorophore-spacer-receptor motif with two thiourea receptor, the primary nitrogen as a spacer and the allyl group as the fluorophore. The receptor was characterised by ^{1}H-NMR and UV-Vis spectroscopic techniques to confirm the structural facets. The structure of receptor **A** is characterised by two absorption peaks (Figure 12), the main peak at 270 nm and a weak shoulder peak at 316 nm which could be due to the ICT transitions of the thiourea moiety and the excitation of the π electrons in the phenyl ring [92,93]. The ^{1}H-NMR results obtained for receptor **A** (Appendix 1.1) shows that the peaks are more downfield (7.12-10.28ppm). The ^{1}H-NMR characteristic features of receptor **A** include δ_H: 10.28 (m, 1H, -CNHAr); 9.80 (s, 1H, -NNH-) 9.08 (s, 4H, -CNHC-), 7.62 (m, 10H,), 7.37 (m, 11H) and 7.12 (m, 6H) (Appendix 1.1).

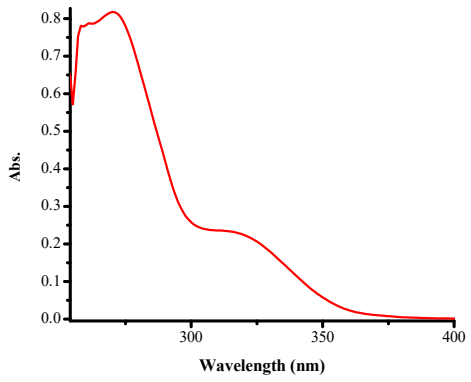

Figure 12. UV-Vis absorption spectrum of free receptor **A** (1 x 10^{-5}M) in DMSO

4.1.2 Visual sensing of different ions

The colorimetric sensitivity of receptor **A** in DMSO towards anions in TBA salts form was visually observed. The results show that no colour change was observed with the addition of these anions: AcO^-, F^-, CN^-, OH^-, Br^-, Cl^-, ClO_4^-, HSO_4^-, I^-, N_3^-, NO_3^-, and $H_2PO_4^-$ (Figure 13).

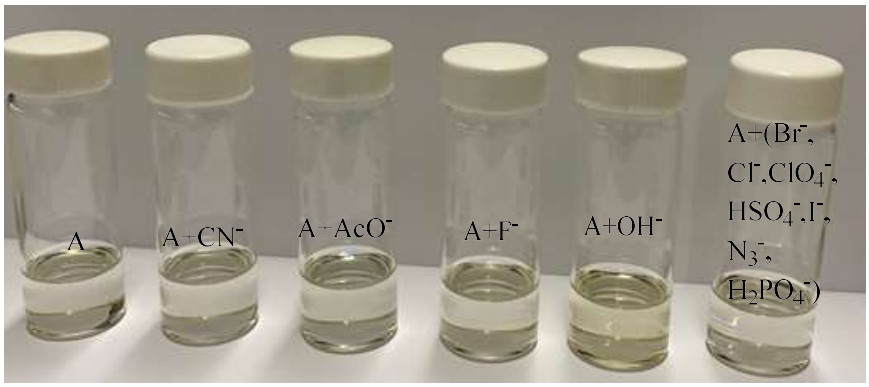

Figure 13. Colour change of receptor **A** ($1x10^{-3}$M) in DMSO upon interaction with anions.

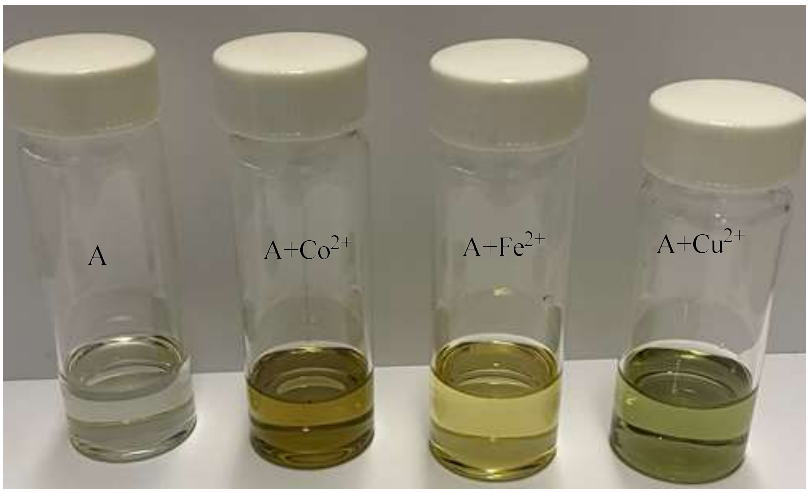

Figure 14. Colour changes of receptor **A** ($1x10^{-3}$M) in DMSO upon interaction with cations.

Equally, colorimetric sensitivity of receptor **A** towards cations such as Cu^{2+}, Fe^{2+}, Ag^{+}, Al^{3+}, Cd^{2+}, Co^{2+}, Cr^{3+}, Mg^{2+}, Mn^{2+}, Pb^{2+}, Ni^{2+}, Sn^{2+}, Sr^{2+} and Zn^{2+} was also observed in DMSO. Among the cations investigated, only Cu^{2+}, Fe^{2+} and Co^{2+} depicted colour change. The addition of copper ion resulted in the colour change from colourless to green, while with cobalt, the colour changed from colourless to brown and iron colourless to light yellow (Figure 14). Receptor **A** was able to visually discriminate the different cations from each other with each cation displaying a unique colour change. However, no colour change was observed in all the other anions and cations.

4.1.3 Absorption spectra of receptor A with different anions

The binding ability of receptor **A** with anions was investigated using UV-Vis spectroscopy in DMSO with TBA salts solutions of AcO^{-}, Br^{-}, Cl^{-}, ClO_4^{-}, CN^{-}, F^{-}, HSO_4^{-},I^{-}, N_3^{-}, NO_3^{-}, OH^{-} and $H_2PO_4^{-}$ (0.03M) at ambient temperature. The titration was carried out using an addition of incremental amount of 0.1 molar equivalent to a maximum of 3.0 molar equivalent of each anion to the receptor **A** ($1x10^{-5}$ M) solution. The molar addition of AcO^{-}, F^{-}, CN^{-} and OH^{-} caused a bathochromic shift of the absorption maxima 316 nm from 270 nm (Figure 15). The bathochromic shift observed is associated with a π-π^* due to the ICT between the proton of the thiourea N-H and the anions [92]. Furthermore, there exists a strong hydrogen bonding interaction between receptor **A** and the anions (AcO^{-}, F^{-}, CN^{-} and OH^{-}). A well-defined isosbestic point at 286 nm is also observed and it indicates the presence of a complex in equilibrium with receptor **A**.

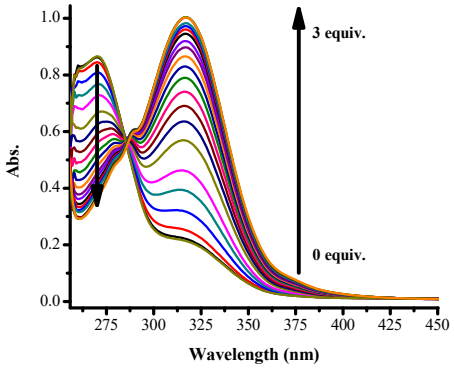
Abs.
Wavelength (nm)
3 equiv.
0 equiv.

(a)

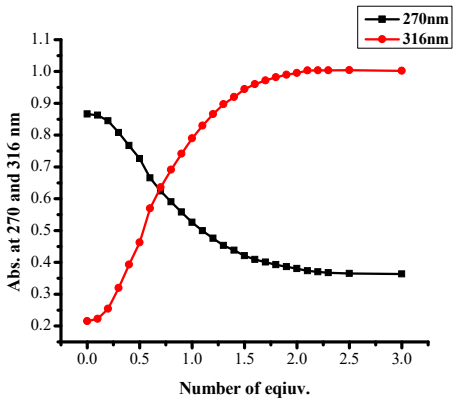
270nm
316nm
Abs. at 270 and 316 nm
Number of eqiuv.

(b)

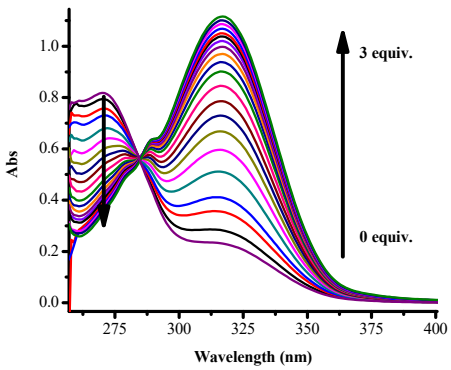
Abs
Wavelength (nm)
3 equiv.
0 equiv.

(c)

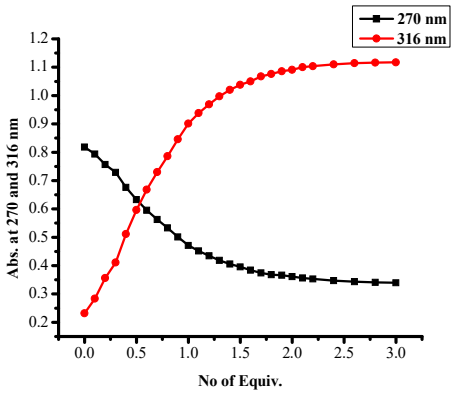
270 nm
316 nm
Abs. at 270 and 316 nm
No of Equiv.

(d)

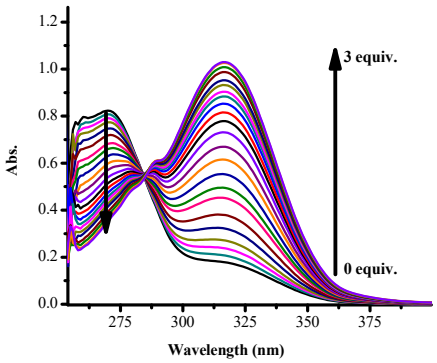
Abs.
Wavelength (nm)
3 equiv.
0 equiv.

(e)

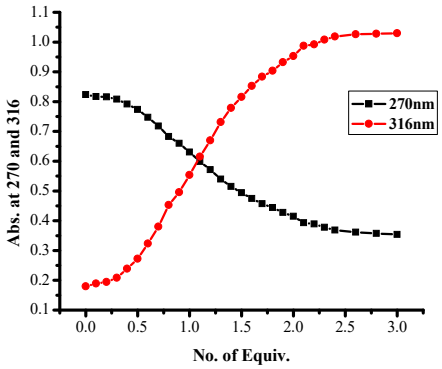
270nm
316nm
Abs. at 270 and 316
No. of Equiv.

(f)

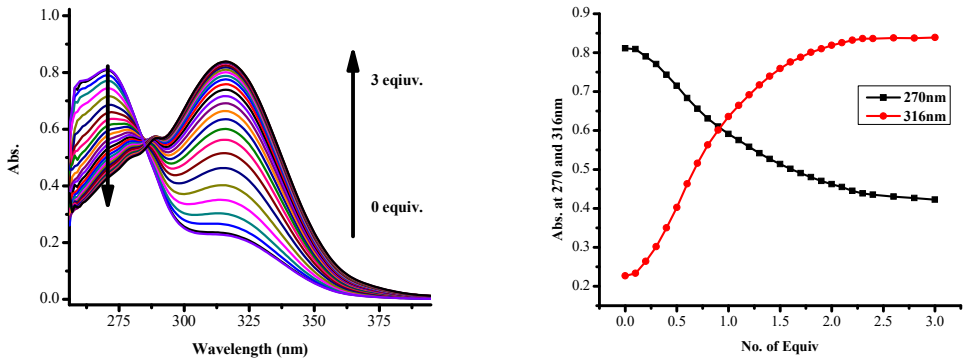

(g) (h)

Figure: 15 The UV-Vis titration spectra and titration profiles of receptor **A** (1 x 10^{-5}M) in DMSO upon addition of 0-3equiv (a,b) CN^-, (c,d) AcO^-, (e,f) F^- and (g,h) OH^- at ambient temperature.

Titration with Br^-, Cl^-, ClO_4^-, HSO_4^-, I^-, N_3^- and $H_2PO_4^-$ yield no significant UV-Vis spectral changes (Figure S1). The 3 equivalent spectra of AcO^-, F^-, CN^- and OH^- were plotted in one graph to compare their sensitivity towards receptor **A**. From the plot, AcO^- has the highest peak followed by F^-, then CN^- and OH^- being the lowest (Figure 16). Furthermore, 3 equivalent spectra of each anion were combined in one plot to compare their sensitivity towards receptor **A** as shown in Figure 17 below.

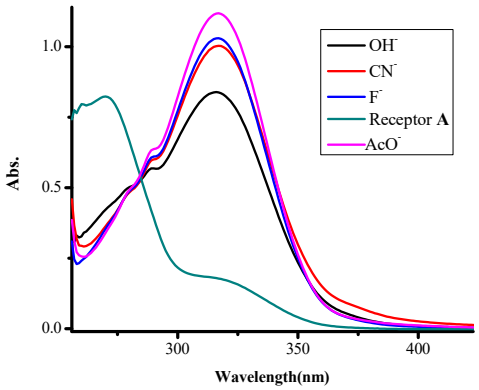

Figure 16. UV-Vis absorption spectra of receptor **A** in the presence of acetate, fluoride, cyanide and hydroxide.

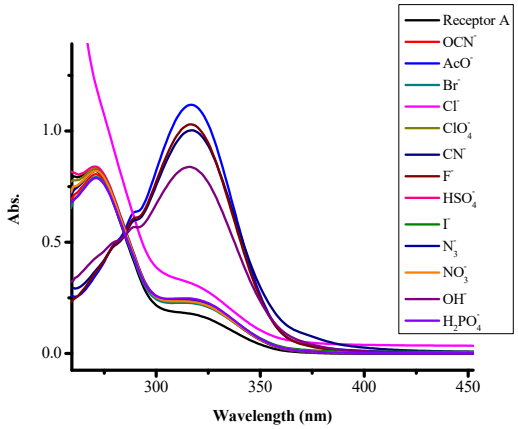

Figure 17. The UV-Vis spectral of receptor **A** (1×10^{-5}M) upon titration with solution of anions (AcO^-, Br^-, Cl^-, ClO_4^-, CN^-, F^-, HSO_4^-, I^-, N_3^-, NO_3^-, OH^- and $H_2PO_4^-$) in DMSO at ambient temperature.

4.1.4 UV-Vis titration of receptor A with cations

The interaction of receptor **A** was also investigated with metal chloride salts or metal nitrate salts. The presence of soft donor atoms such as sulphur, oxygen and nitrogen made it possible for receptor **A** to interact with cations through coordination. The chloride and nitrate salts used are: $FeCl_2{\cdot}4H_2O$, $SnCl_2{\cdot}2H_2O$, $CrCl_3{\cdot}6H_2O$, $MgCl_2$, $MnCl_2{\cdot}4H_2O$, $CuCl_2{\cdot}2H_2O$, $CdCl_2{\cdot}H_2O$, $SrCl_2{\cdot}6H_2O$, $AlCl_3$, $Ni(NO_3)_2{\cdot}6H_2O$, $AgNO_3$, $Hg(NO_3)_2{\cdot}H_2O$, $Zn(NO_3)_2{\cdot}6H_2O$, $Co(NO_3)_2{\cdot}6H_2O$, $Pb(NO_3)_2$, and $Fe(NO_3)_3{\cdot}9H_2O$ (0.03M) at ambient temperature. Figure 18a-c- indicates the change in the UV-Vis spectra of receptor **A** ($1x10^{-5}$M) upon addition of salts of Cu^{2+}, Fe^{2+} and Co^{2+}; these cations interacted with the receptor **A** through coordination. Titration with Sn^{2+}, Cr^{3+}, Mg^{2+}, Mn^{2+}, Cd^{2+}, Sr^{2+}, Al^{3+}, Ni^{2+}, Ag^{+}, Hg^{2+} and Zn^{2+} yield no significant UV-Vis spectra changes (Figure S2).

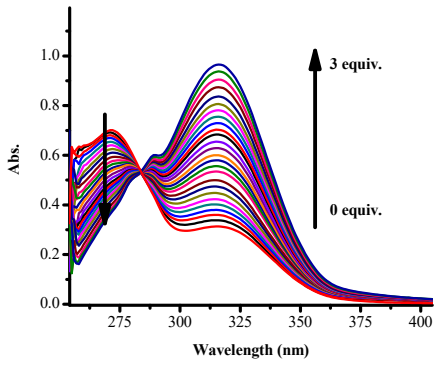

(a)

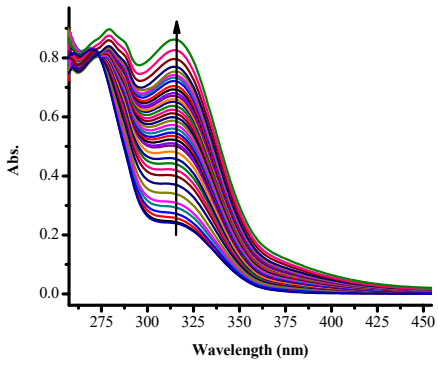

(b)

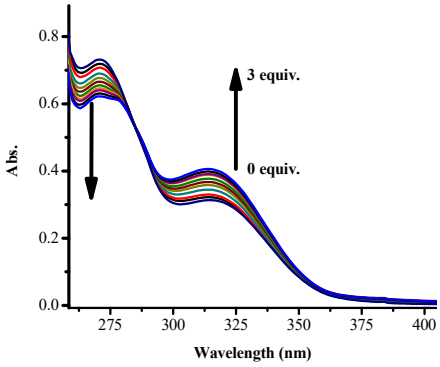

(c)

Figure 18. The UV-Vis titration spectral changes of receptor **A** (1 x 10^{-5}M) with (a) Cu^{2+}, (b) Fe^{2+} and (c) Co^{2+}in DMSO upon addition of 0-3 equiv. (a) Cu^{2+}, (b) Fe^{2+} and (c) Co^{2+} at ambient temp.

The molar addition of cations Cu^{2+}, Fe^{2+} and Co^{2+} also caused a bathochromic shift. The molar addition of copper resulted in an absorption peak centered at 270 nm disappearing concomitantly with the appearance of the peak at 316 nm (Figure 18a). For cobalt, the absorption peak at 270 nm disappearing concurrently with the new peak formed at 316 nm (Figure 18c). A well-defined isosbestic point is observed for Cu^{2+} and Co^{2+} at 284 nm, and the formation of an isosbestic point for copper and cobalt indicates that a complex is formed with the sensor. However, iron behaves differently with a new peak at 315 nm appearing parallel to the sensor peak at 270 nm, and no isosbestic point was observed (Figure 18b). Furthermore, receptor **A** is more sensitive and selective to copper than iron and cobalt (Figure 19), the comparison of different cation sensitivity (Figure 20).

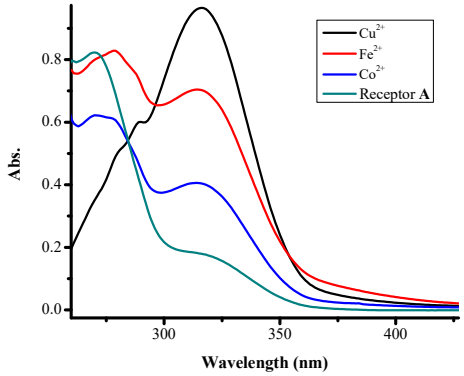

Figure 19. UV-Vis absorption spectra of receptor receptor **A** in the presence of copper, iron and cobalt ions.

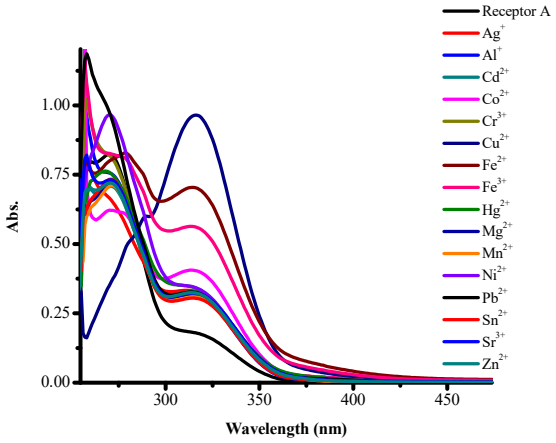

Figure 20. The absorption spectral of receptor **A** (1 x 10^{-5}M) upon titration with solution of cations (Ag^{+}, Al^{3+}, Cd^{2+}, Co^{2+}, Cr^{3+}, Mg^{2+}, Mn^{2+}, Pb^{2+}, Ni^{2+}, Sn^{2+}, Sr^{2+}, Zn^{2+}) in DMSO at ambient temperature.

4.1.5 Job plot studies of receptor A with ions

The Job plot was used to determine the stoichiometric ratios between receptor **A** and the anions. The Job plot of the UV-Vis titrations of anions with the concentration of 10µl was performed to explore the binding mechanism of anions with the receptor **A.** The total concentration of receptor **A** and anions was (1 x 10^{-4}M) with various molar fraction from 1µl to 10µl with incremental of 1µl [sensor]/ [sensor] + [anion]. The data obtained from the jobs plot spectra indicate that there are variations in the interaction ratio of anions and the receptor **A**. The ratios vary from 3:1 to 1:1 ratio with the selected anions. The presence of NH which possesses the acidic protons made receptor **A** an ideal sensor for anions. The proposed mode of interaction for anions is through hydrogen bonding (Scheme 5). The interaction of acetate has maximum absorption at 7 molar fraction which indicates that **A**-AcO form a 1:3 complex, (1**A:** 3AcO) (Figure 21a). Fluoride and hydroxide have similar interaction with a maximum absorption observed at 5 molar fraction, which means that **A**-F and **A**-OH form stoichiometric ratio of 1:1 complex (Figure 21b and d)**.** For cyanide, the maximum absorption was observed at 6 molar fraction which indicate that **A**-CN form a 1:2 complex (Figure 21c).

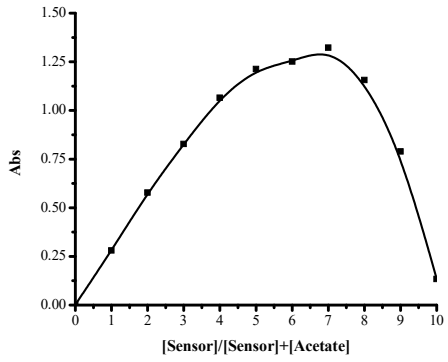

(a)

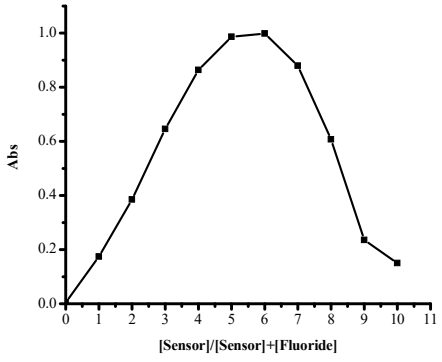

(b)

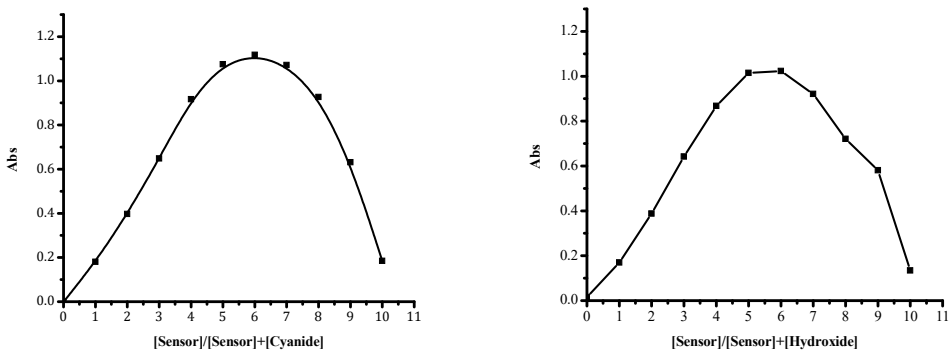

(c) (d)

Figure 21. The Job plots of (a) [**A**-AcO$^-$], (b) [**A**-F$^-$], (c) [**A**-CN$^-$], and (d) [**A**-OH$^-$] at 1 x 10^{-4} M in DMSO.

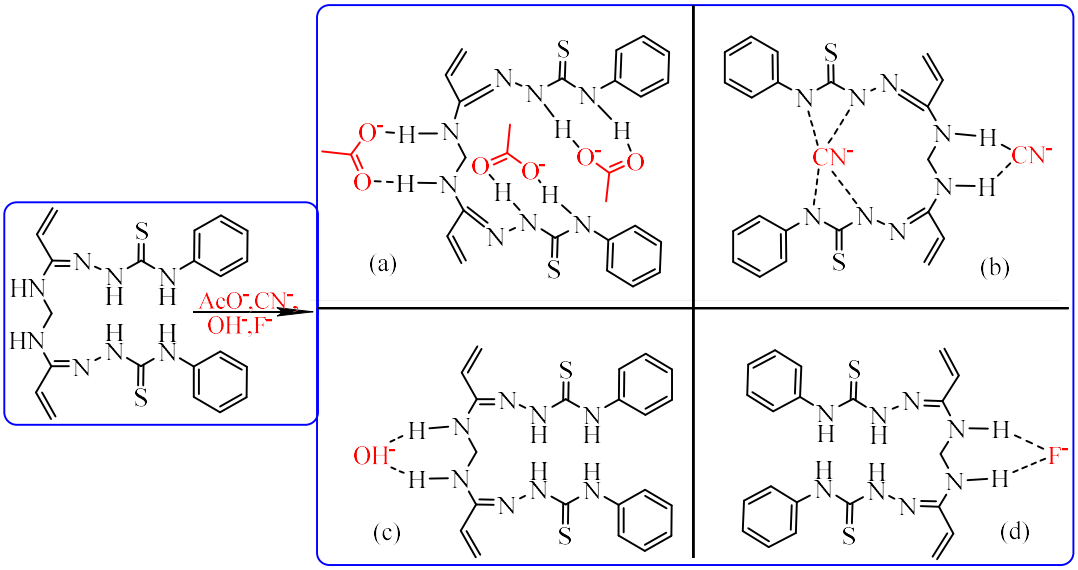

Scheme 5: Proposed binding models of (a) **A**-AcO, (b) **A**-CN, (c) **A**-OH and (d) **A**-F

To determine the binding mechanism for cations with the receptor **A**, Job's plot of the UV-Vis titrations was performed. The total concentration of receptor **A** and cations was (1 x 10^{-4}M) with various molar fraction [sensor]/ [sensor] + [cation]. The obtained spectra show that for receptor **A-**copper, a maximum absorption was observed at 5 molar fraction which indicates that [**A-Cu]** form a 1:1 complex (Figure 22a). Iron has a different stoichiometric ratio from copper, and for the receptor **A-**iron, a maximum absorption was observed at 9 molar fraction, which means that receptor **A-** iron form 9:1 complex (Figure 22b). For receptor **A**-cobalt, a maximum absorption is observed at 9 molar fraction, forming a 9:1 complex (Figure 22c)**.** The proposed binding modes of the sensor and cations were deduced from the Job plot results (Scheme 6). The interaction of receptor **C** and cations is based on coordination through the donor atoms nitrogen and sulphur. From the Job's plot and absorption spectra of iron depicted, a broad band and no isosbestic point was observed, and it is likely that A-Fe interaction is through π-π starking.

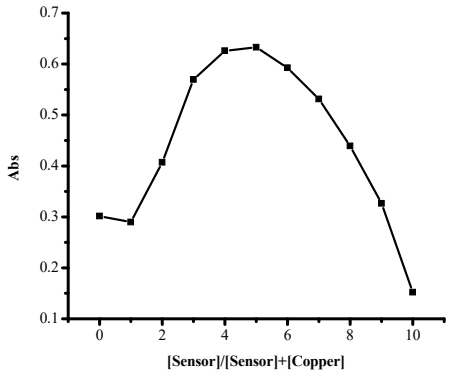

(a)

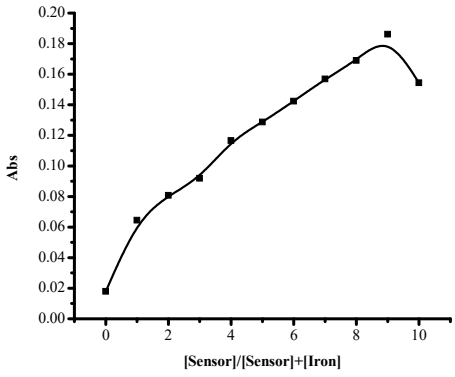

(b)

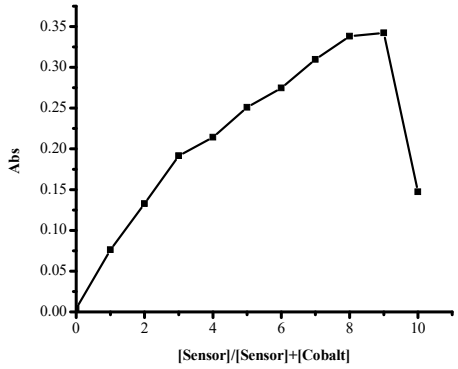

(c)

Figure 22. Job plots of (a) [A-Cu^{2+}], (b) [A-Fe^{2+}] and (c) [A-Co^{2+}] at 1 x 10^{-4} M. in DMSO.

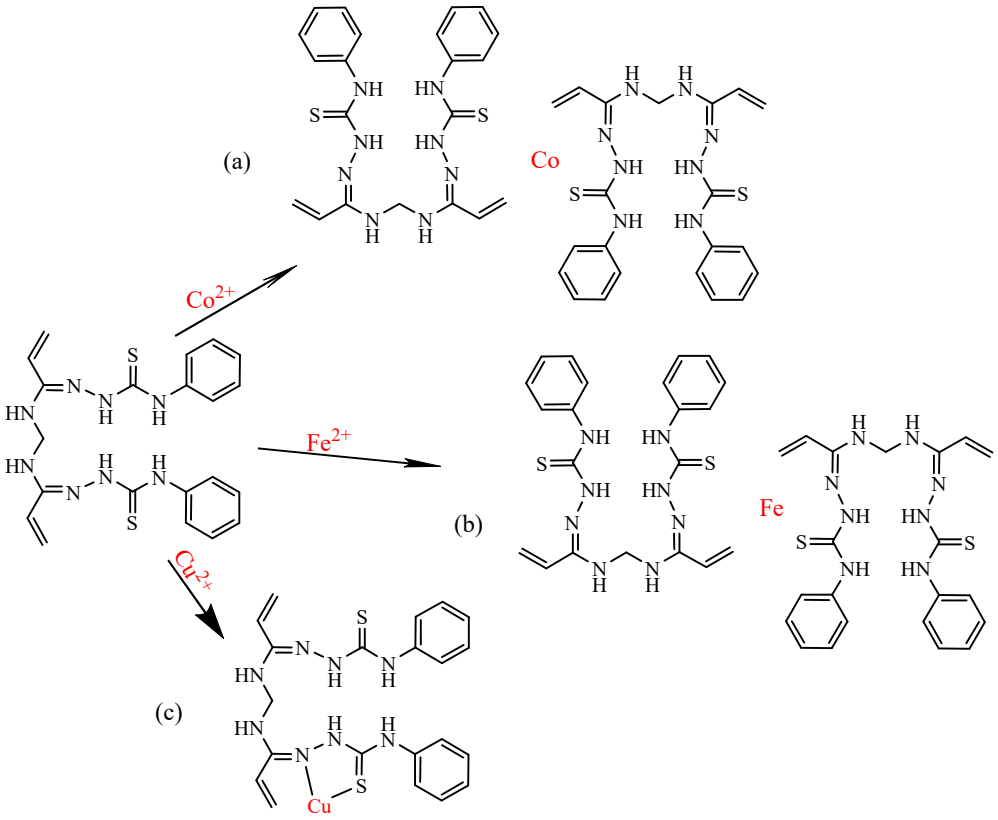

Scheme 6: Proposed binding models of (a) **A-**Co, (b) **A-**Fe and (c) **A-**Cu.

4.1.6 Fluorescence titration of receptor A with ions

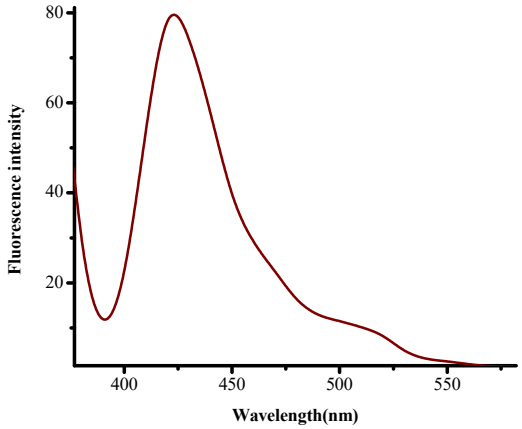

Figure 23. Fluorescence of the receptor **A**

The fluorophore probes redesign in a way that the structure bears the donor atoms such as nitrogen, sulphur, and oxygen with a function of coordinating to metal ions. Whereas, the existence of the amine group on receptor **C** made it capable of interacting with the anions through hydrogen bonding/deprotonation. Receptor **A** may offer up to three donor atoms, namely the thioamide nitrogen, the imine nitrogen and sulphur. The receptor is expected to be deprotonated for it to coordinate with the cations. The receptor **A** displayed a strong fluorescence emission band at 423 nm (Figure 23) with the excitation wavelength at 370 nm observed from the fluorescence spectroscopy. Moreover, host-guest recognition ability was further investigated with fluorescence titration in DMSO. Anions 0-3 molar equiv. were used in the fluorescence titrations and receptor **A** ($1x10^{-5}$M). Several anions that are recognized via UV-Vis titration were explored with the fluorescence spectroscopy

which include TBA salts solutions of AcO^-, CN^-, F^- and OH^- at ambient temperature. The molar addition of 3 equiv. of each of these AcO^-, F^-, CN^- and OH^- resulted in fluorescence enhancement of the emission spectrum figure (24a and b-25a and b). For AcO^- and CN^-, the enhancement of emission is associated with a red shift from 421 nm to 438 nm (Figure 24a and b), whereas for F^- and OH^-, the emission enhancement is shifted from 420 nm to 435 nm (Figure 25a and b). Generally, for the anion, fluorescence behaved in a similar way.

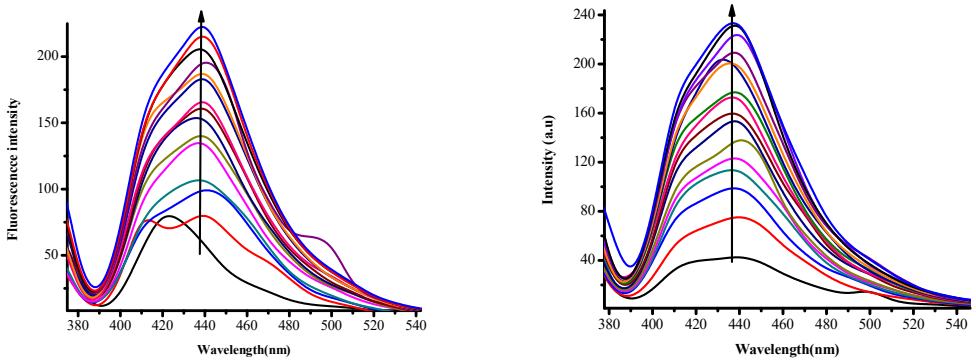

(a) (b)

Figure 24. Fluorescence titration spectra of receptor **A** (1 x 10^{-5}M) in DMSO (3.0µl) in the presence of increasing amounts of 0-3 equiv. (a) AcO^- and (b) CN^-

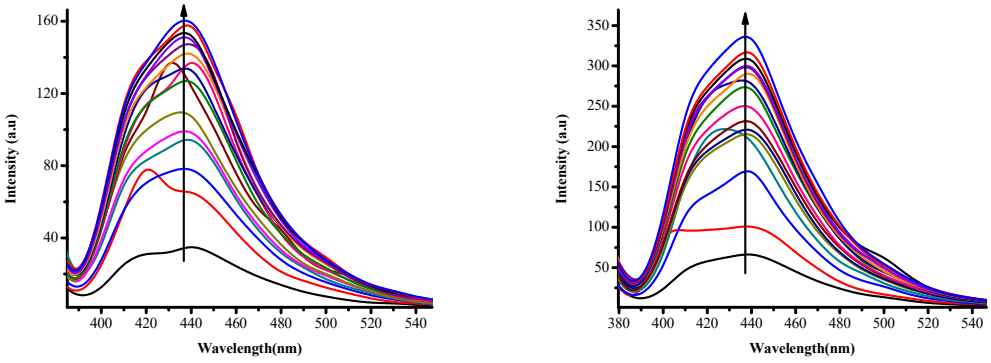

(a) (b)

Figure 25. Fluorescence titration spectra of receptor **A** (1 x 10^{-5}M) in DMSO (3.0µl) in the presence of increasing amounts of 0-3equiv (a) F^- (b) OH^-.

Similarly, the same fluorescence test was conducted for metal ions. The addition of 10 molar equiv. iron to receptor **A** emission quenching was observed in the region of 430 nm (Figure 26a). The fluorescence titration of mercury and copper with receptor **A** resulted in a slight enhancement of the emission; for mercury and copper a broad band is observed in the region 436 nm as shown in the (Figure 26b and 27). The addition of both 10 molar equiv. nickel and 10 molar equiv. cobalt resulted in the enhancement of the emission in the region of 435 nm respectively (Figures 26c and 26d).

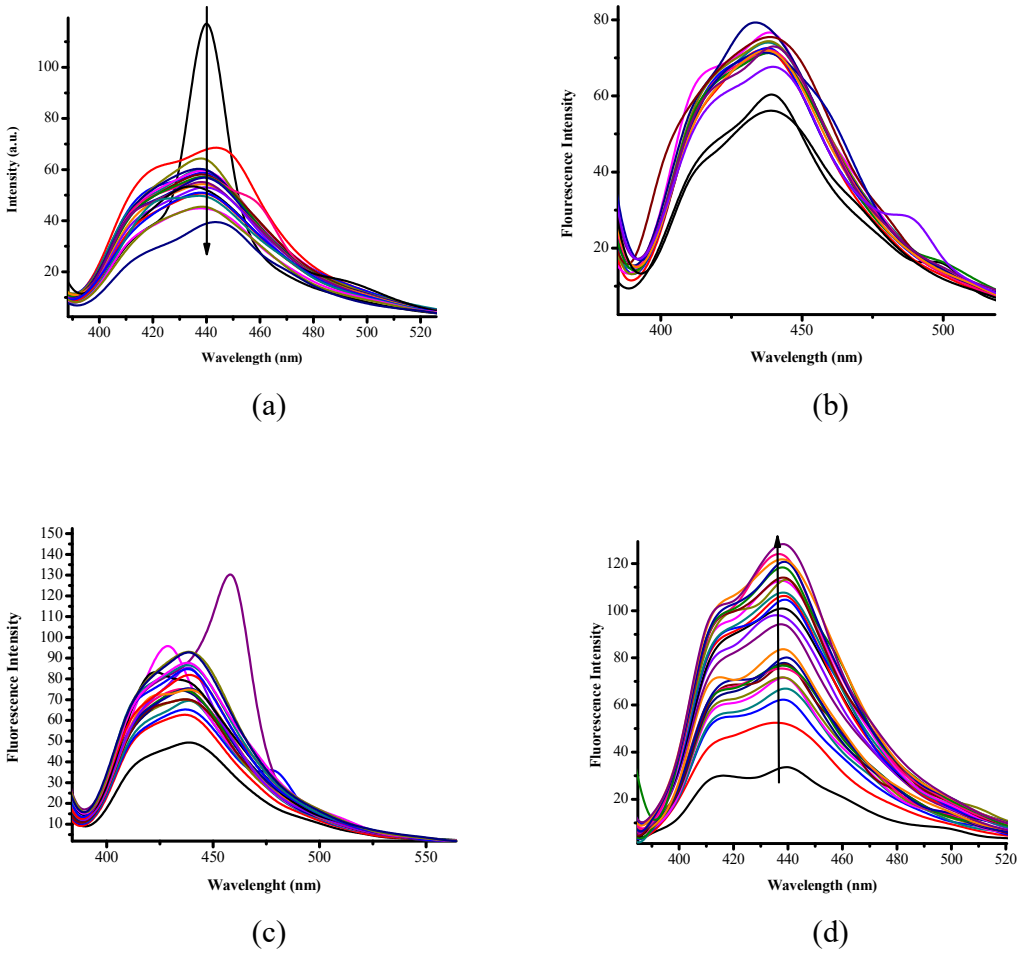

Figure 26. Fluorescence titration spectra of receptor **A** (1 x 10^{-5}M) in DMSO (3.0µl) in the presence of increasing amounts of 0-10equiv (a) Fe^{2+}, (b) Hg^{2+}, (c) Ni^{2+} and (d). Co^{2+}.

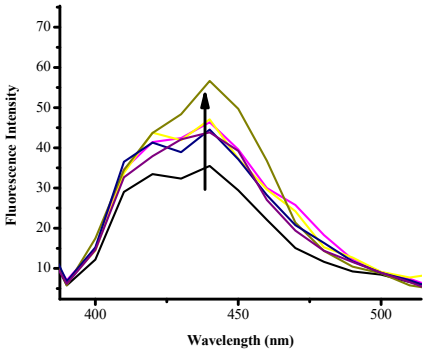

Figure 27. Fluorescence spectra of receptor **A** (1 x 10^{-5}M) in DMSO (3.0µl) in the presence of increasing amounts of 0-1 equiv. Cu^{2+}.

4.2 Receptor C interaction with ions

4.2.1. Characterization of receptor C

The receptor **C** has been synthesized by Schiff base condensation reaction. The design of this sensor is based on fluorophore-spacer-receptor, with naphthol fluorophore separated by a methylene spacer and hydrazinecarbodithioic acid as a receptor. The sensor has an electron withdrawing naphthol and electron donating N-H. The receptor was characterised by UV-Vis and ^{1}H-NMR spectroscopic techniques to confirm the structural aspects. The structure of receptor **C** (Figure 28) is characterised by several absorption bands at 266 nm, 337 nm, 384 nm, with a shoulder peak at 402 nm and 489 nm. Two prominent peaks at 266 nm and 384 nm were observed among the several absorption peaks. The receptor has absorptions bands in both the UV and the visible region. The absorption band in the shorter wavelength regions are ascribed to the π-π* transitions whereas the longer wavelengths are ascribed to the intermolecular charge transfer. The peak at 489 nm in the low energy

region is ascribed to the visible light induced charge transfer. The ^{1}H-NMR was recorded in DMSO-d_6 at 400 MHz. The ^{1}H-NMR characteristic features of receptor **C** appear more downfield (7.23-13.37ppm) in the spectrum include δ_H:13.37(s,1H, -OH), 11.06 (s,1H, -NH-), 9.21 (s,1H, H^7) 8.76 (d, *J*=8.58Hz,1H,H^1), 7.94 (d, *J*=8.94Hz,1H, H^5), 7.87 (d, *J*=7.62Hz, 1H, H^4), 7.59 (ddd, *J*= 1.32Hz, *J*=6.93Hz,*J*=8.46Hz, 1H, H^3), 7.40 (m, 1H,H^2) and 7.23 (d, *J*=8.94,1H, H^6) (Appendix 1.2).

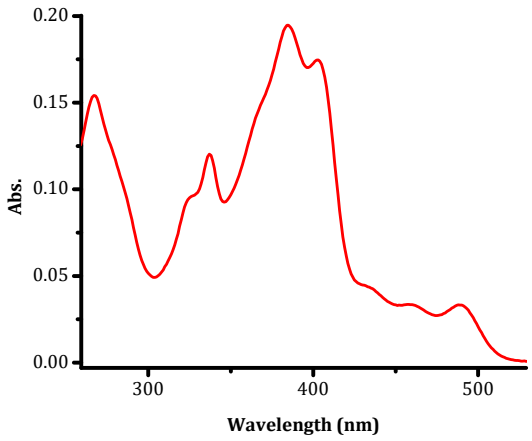

Figure 28. UV-Vis absorption spectrum of free receptor **C** (1 x 10^{-5}M) in DMSO.

4.2.2 Visual sensing of ions

The colorimetric sensing ability of receptor **C** (1 x 10^{-4}M) in DMSO was monitored with a naked eye before and after the addition of TBA salts, displaying colour changes (Figure 29). For AcO^-, F^-, OCN^-, CN^-, OH^-, N_3^- and $H_2PO_4^-$, colour changed from light yellow to yellow indicating a chemical interaction between the sensor and the anions, whereas for

the addition of Br^-, Cl^-, $ClO4^-$, HSO_4^-, I^-, and NO_3^-, no detectable colour change was observed.

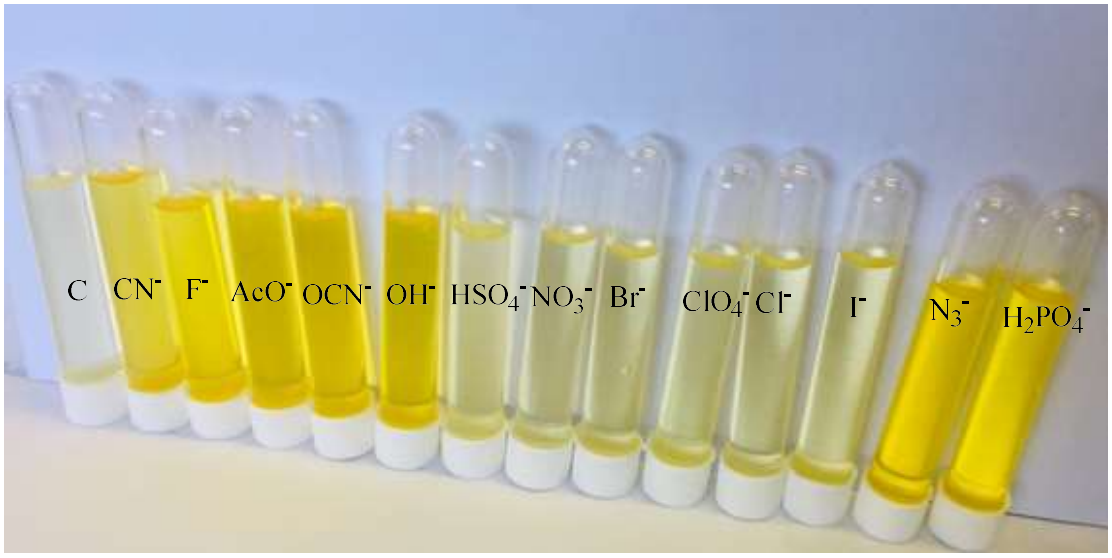

Figure 29. Colour change of receptor **C** ($1x10^{-4}$M) in DMSO upon interaction with anions

Similarly, colorimetric sensitivity of receptor **C** towards cations, such as Cu^{2+}, Fe^{2+}, Ag^+,Al^{3+}, Cd^{2+}, Co^{2+}, Cr^{3+}, Mg^{2+}, Mn^{2+}, Pb^{2+},Ni^{2+}, Sn^{2+},Sr^{2+} and Zn^{2+}, was also tested in DMSO. Upon investigation, receptor **C** depicted colour change with several metal ions (Figure 30). With addition of nickel, the colour changed from light yellow to yellow, and iron colour changed to brown. With addition of mercury, the colour changed slightly from light yellow to light green and zinc colour changed from light yellow to yellow and copper changed the colour from light yellow to light green. However, no significant colour change was observed with other cations.

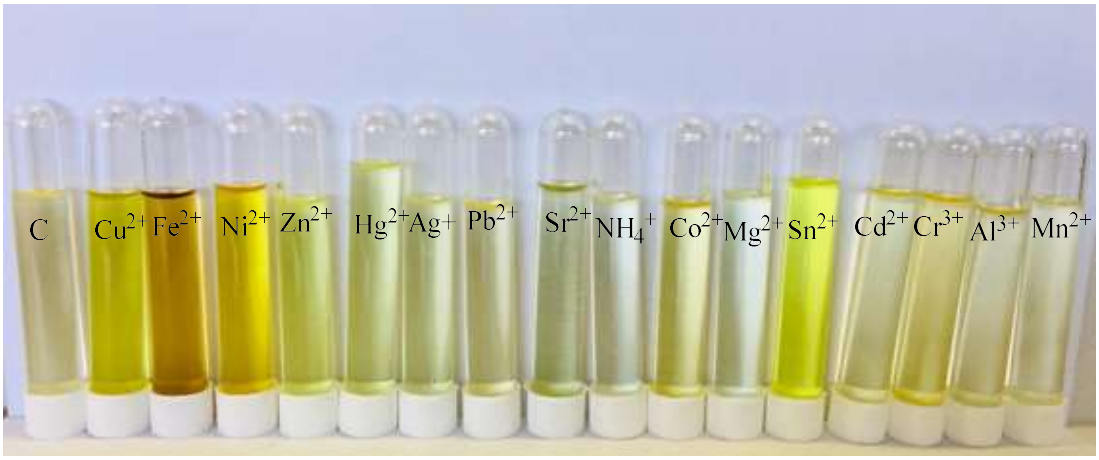

Figure 30. Colour change of receptor C ($1x10^{-4}$M) in DMSO upon interaction with cations.

4.2.3 UV-Vis titration of receptor C with anions

The recognition ability of receptor **C** was investigated with TBA salts solutions of AcO^-, Br^-, Cl^-, ClO_4^-, CN^-, F^-, HSO_4^-, I^-, N_3^-, NO_3^-, OH^- and $H_2PO_4^-$ (0.03) at ambient temperature. Figure (31a-e and 32a, b) indicates the change in the UV-Vis spectra of receptor **C** ($1x10^{-5}$M) upon addition of salts of OCN^-, CN^-, AcO^-, F^-, OH^- and $H_2PO_4^-$, respectively. Titration with Br^-, Cl^-, ClO_4^-, HSO_4^-, I^-, and $H_2PO_4^-$ yield no significant UV-Vis spectra changes (Figure S3).

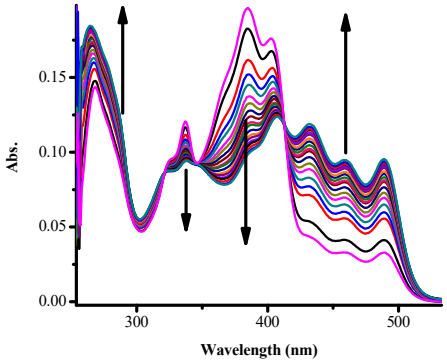
Abs.
0.00
0.05
0.10
0.15
300
400
500
Wavelength (nm)

(a)

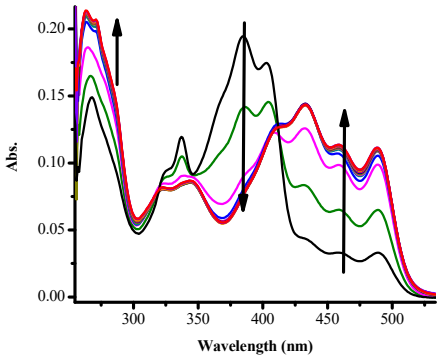
Abs.
0.00
0.05
0.10
0.15
0.20
300
350
400
450
500
Wavelength (nm)

(b)

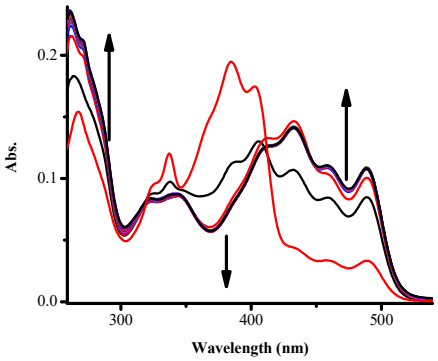
Abs.
0.0
0.1
0.2
300
400
500
Wavelength (nm)

(c)

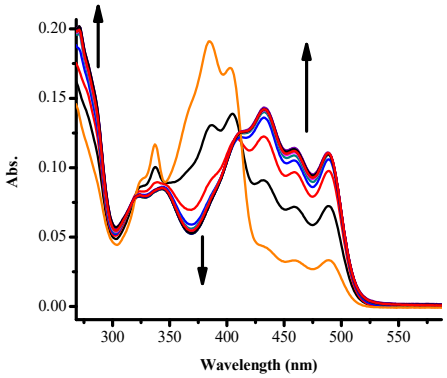
Abs.
0.00
0.05
0.10
0.15
0.20
300
350
400
450
500
550
Wavelength (nm)

(d)

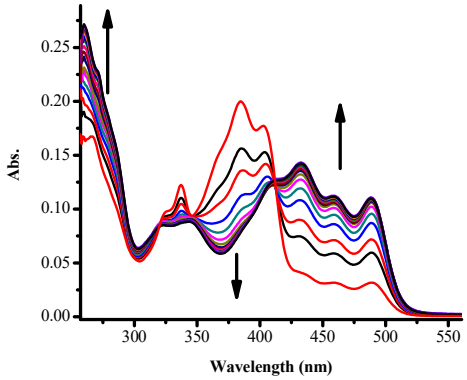

(e)

Figure 31. The UV-Vis titration spectral changes of receptor **C** (1 x 10^{-5}M) with OCN^- in DMSO upon addition of 0-3equiv (a) OCN^-, (b) CN^-, (c) AcO^-, (d) F^- and (e) OH^- at ambient temperature.

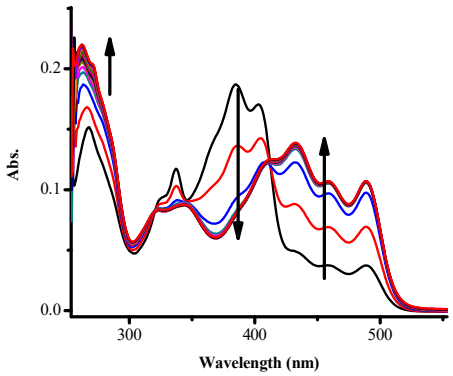

(a)

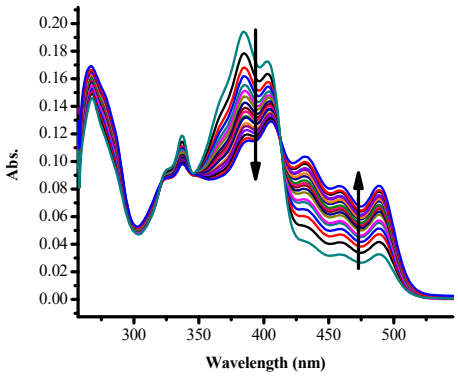

(b)

Figure 32. The UV-Vis titration spectral changes of **C** receptor (1 x 10^{-5}M) with. (a) $H_2PO_4^-$ and (b) N_3^- in DMSO upon addition of 0-2.5equiv $H_2PO_4^-$ and N_3^- at ambient temperature.

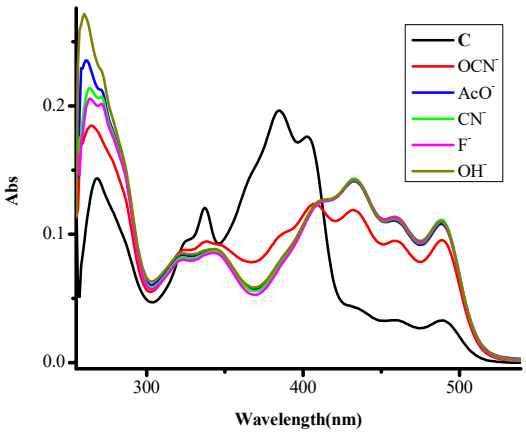

Figure 33. Receptor **C** and responding anions (3 equiv.)

The addition of AcO^-, CN^-, F^-, OCN^- and OH^- caused a bathochromic shift from 384 nm and its shoulder peak at 402 nm, as well as the peak at 337 nm disappearing and forming new peaks at 432 nm and 459 nm, respectively. In addition, the peak at 489 nm become more distinctive, whereas for the peak at 266 nm is enhanced. The bathochromic shift observed is associated with a π-π*/n- π*; this is due to intermolecular charge transfer between the proton of the hydrazone and the anions. The sensitivity of the anions with the receptor C is displayed (Figure 33) by comparing the 3 equiv. spectra of the 5 anions (OCN^-, AcO^-, F^-, CN^- and OH^-) that are sensing, with cyanide ion being more sensitive, than fluoride, hydroxide acetate and cyanate being the least.

4.2.4 UV-Vis titration of receptor C with cations

The recognition ability of receptor **C** was investigated with metal salts. The chloride and nitrate salts used are: $FeCl_2{\cdot}4H_2O$, $SnCl_2{\cdot}.2H_2O$, $CrCl_3{\cdot}6H_2O$, $MgCl_2$, $MnCl_2{\cdot}.4H_2O$,

$CuCl_2 \cdot 2H_2O$, $CdCl_2 \cdot H_2O$, $SrCl_2 \cdot 6H_2O$, $AlCl_3$, $Ni(NO_3)_2 \cdot 6H_2O$, $AgNO_3$, $Hg(NO_3)_2 \cdot H_2O$, $Zn(NO_3)_2 \cdot 6H_2O$, $Co(NO_3)_2 \cdot 6H_2O$, $Pb(NO_3)_2$, $Fe(NO_3)_3 \cdot 9H_2O$ at room temperature. Figure (34a-e) indicates the change in the UV-Vis absorption spectra of receptor **C** ($1x10^{-5}$M) upon addition of salts of Cu^{2+}, Fe^{2+}, Ni^{2+}, Zn^{2+} and Hg^{2+}. Upon the addition of Cu^{2+}, the prominent peak at 384 nm disappeared concurrently with the appearance of a peak at 433 nm and a broad band in the region around 300 nm. Two isosbestic points were observed at 355 nm and 413 nm, indicating the presence of a complex in equilibrium with receptor **C**. The interaction of Cu^{2+} and receptor **C** is ascribed to charge transfer induced by coordination (Figure 34a). The addition of Fe^{2+} caused a significant decrease of the peak at 384nm with the formation of a band in the 300 nm region, and no isosbestic point could be observed (Figure 34b.). Upon the addition of Ni^{2+}, the peak at 384 nm disappeared simultaneously with the appearance of a peak at 438 nm. Two well-defined isosbestic points were observed with Ni^{2+} at 331 nm and 413 nm; the interaction with receptor is attributed to coordination just like Cu^{2+} (Figure 34c.). Furthermore, the addition of Zn^{2+} to receptor **C** resulted in the disappearance of the peak at 384 nm concurrently with the appearance of a peak at 442 nm. Two isosbestic points were observed; however, only one isosbestic was well defined at 411 nm and the one in the region 342 nm was not well defined (Figure 34d). Upon the addition of Hg^{2+}, a new band in the region 439 nm appeared simultaneously with the disappearance of the peak at 384 nm. Two isosbestic points were observed with Hg^{2+} in the region around 344 nm and 415 nm; however, they are not well defined (Figure 34e). Titration with Sn^{2+}, Cr^{3+}, Mg^{2+}, Mn^{2+}, Cd^{2+}, Sr^{2+}, Al^{3+}, Ag^{+} and Co^{2+} yield no significant UV-Vis spectra changes (Figure S4).

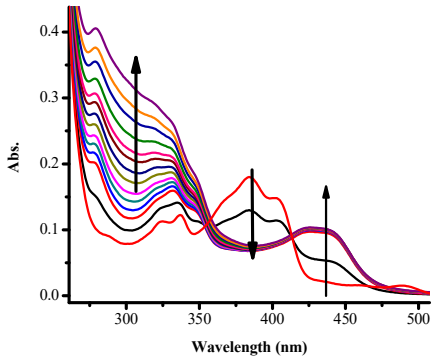
Abs.
Wavelength (nm)

(a)

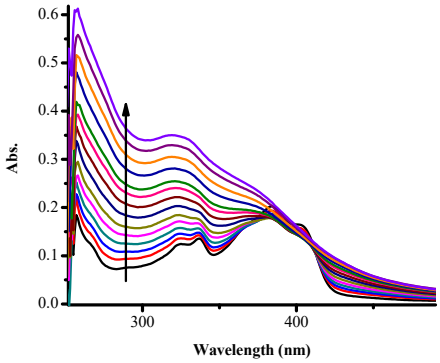
Abs.
Wavelength (nm)

(b)

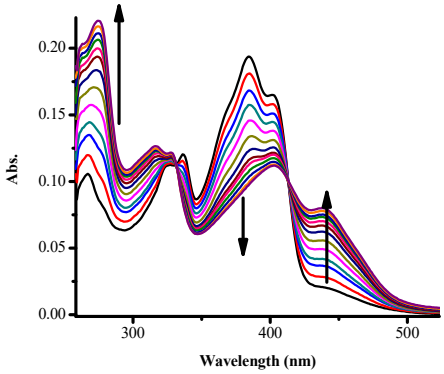
Abs.
Wavelength (nm)

(c)

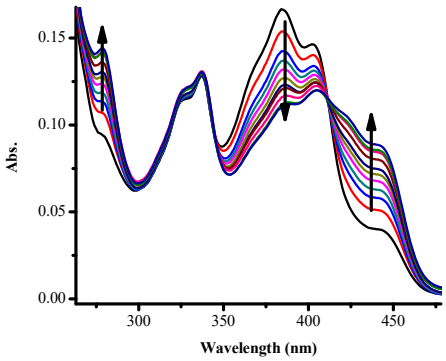
Abs.
Wavelength (nm)

(d)

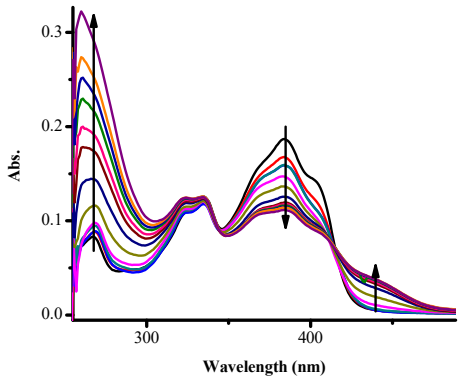

(e)

Figure 34. The UV-Vis titration spectral changes of receptor **C** (1 x 10^{-5}M) with (a) Cu^{2+}, (b) Fe^{2+}, (c) Ni^{2+}, (d) Zn^{2+} and (e) Hg^{2+} in DMSO upon addition of 0-3equiv.(a) Cu^{2+}, (b) Fe^{2+}, (c) Ni^{2+}, (d) Zn^{2+} and (e) Hg^{2+}at ambient temperature.

4.2.5 Job plots

The binding mechanism of receptor **C** with the ions was determined, and Job plot for the UV Vis titration was carried out. The total concentration of receptor **C** and ions was (1 x 10^{-4}M) with various molar fraction [sensor]/ [sensor] + [ion]. For receptor **C**- cyanide, fluoride, cyanate and hydroxide, the maximum absorption was observed at 5 molar fraction, and this indicate that each of the four anions forms a 1:1 complex with receptor **C (**Figure 35a, c, d and e**).** For acetate (Figure 35b) on the other hand, the maximum absorption was observed at 6 molar fractions and it is likely to form 1:1 complex. The Job plot results was used to propose the interaction of mode of the receptor and anions (Scheme 7). The interaction of receptor **C**-F**, C**-OCN**, C**-OH and **C**-AcO is based on

hydrogen bonding, whereas for **C**-CN, it is through nucleophilic addition with the protons from the hydroxyl and the amine on the sensing compound.

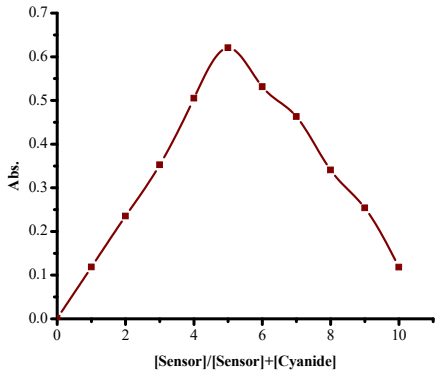

(a)

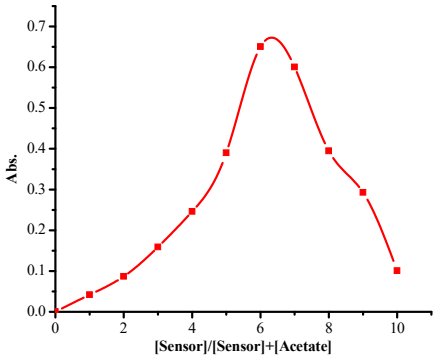

(b)

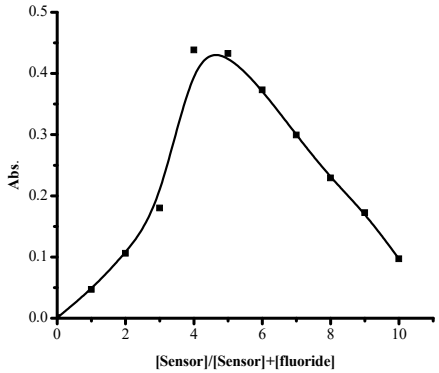

(c)

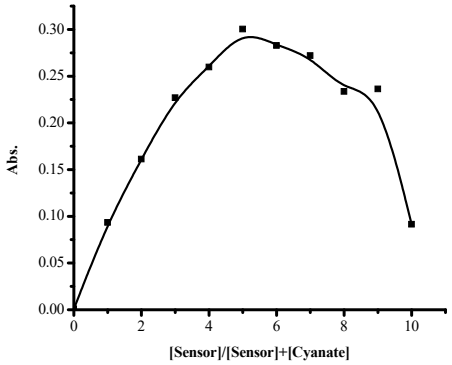

(d)

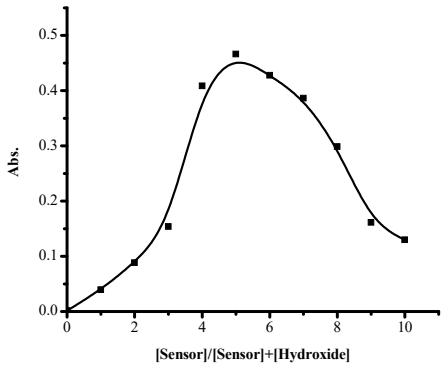

(e)

Figure 35. The Job plots of (a) [**C**- CN], (b) [**C**-AcO], (c) [**C** -F], (d) [**C** -OCN], and (e) [**C** -OH] **C** at 1 x 10-4 M in DMSO.

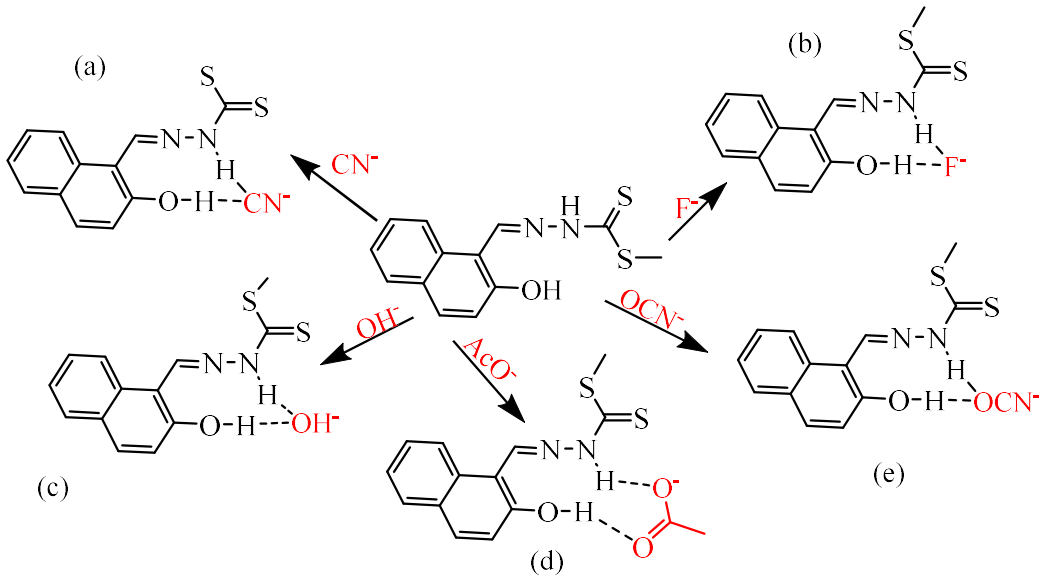

Scheme 7: Proposed binding models of (a) **C**-CN, (b) **C**-F, (c) **C**-OH, (d) **C**-AcO and **C**-OCN

Similarly, to study the binding mechanism of receptor **C** and cations, the Job plot method was used. The obtained spectra show that receptor **C**-copper (Figure 36a) and receptor **C**-zinc (Figure 36d) both have a maximum absorption observed at 6 molar fraction and are likely to each form a 2:1 (2**C**:Cu and 2**C**:Zn) complex with receptor **C**. On the contrary, receptor **C**-iron (Figure 36b) and receptor **C**-nickel (Figure 36c) each has a maximum absorption at 5 molar fraction. Iron and nickel each forms a 1:1 (**C**:Fe and **C**:Ni) complex with receptor **C**. The proposed interactions modes of the sensor and cations were deduced from the Job plot results (Scheme 8). The interaction of receptor **C** and cations is based on coordination through the donor atoms nitrogen, sulphur and oxygen.

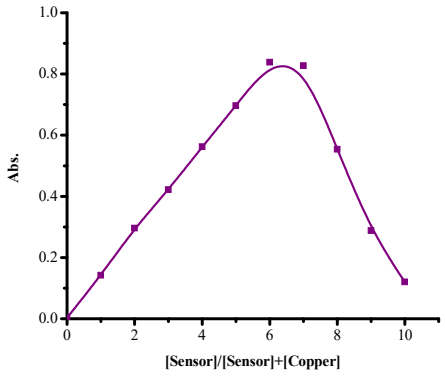

(a)

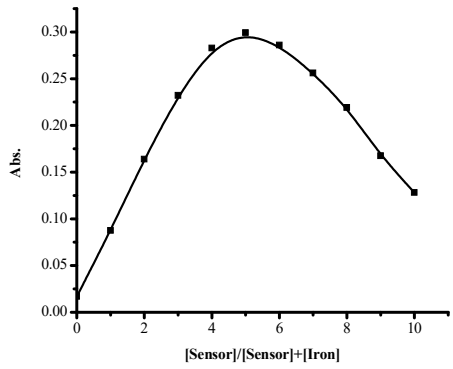

(b)

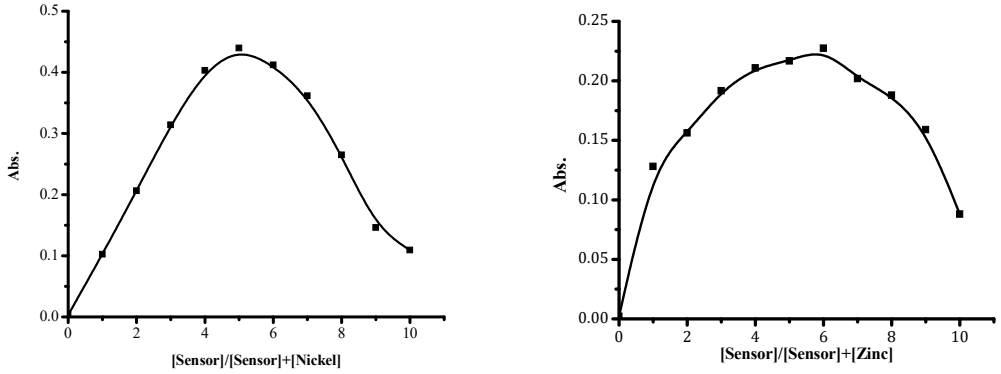

(c) (d)

Figure 36. The Job plots of (a) [**C**-Cu], (b) [**C**-Fe], (c) [**C** -Ni], and (d) [M-Zn] at 1 x 10^{-4} M in DMSO.

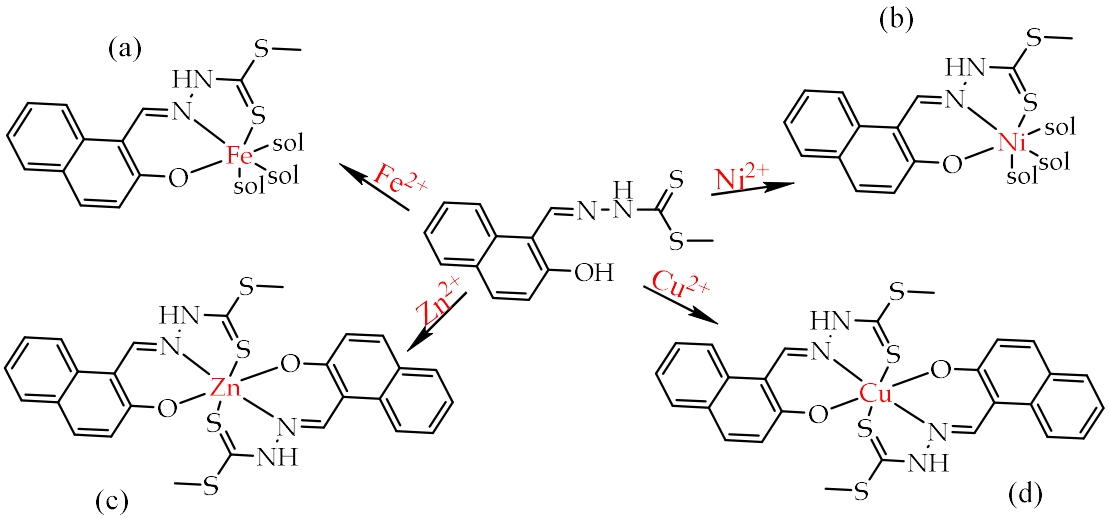

Scheme 8: The proposed binding models of receptor **C** with (a) Fe^{2+}, (b) Ni^{2+}, (c) Zn^{2+} and (d) Cu^{2+}

4.2.6 Fluorescence titration

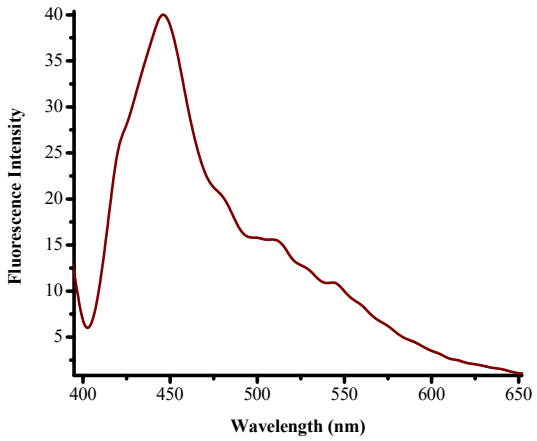

Figure 37. Fluorescence spectra of receptor **C**

The existence of the structural features such as hydroxyl and amine group on receptor **C** made it capable of interacting with the anions. Similarly, the presence of soft donor atoms receptor **C** made it capable of coordinating with the cations. The interactions of receptor **C** with the ionic species have an influence on the ICT, consequently affecting the emission properties of receptor **C**. Receptor **C** was characterized by a peak at 445 nm, and the excitation wavelength of receptor **C** was investigated with fluorescence spectroscopy found to be 390 nm, the fluorescence emission of receptor C (Figure 37). The host-guest recognition ability was further investigated with fluorescence titration in DMSO. Anions and cations were explored with the fluorescence spectroscopy. The anions investigated with the fluorescence spectroscopy are of AcO^-, OCN^-, CN^-, F^- and OH^- at room temperature. The fluorescence spectra of receptor **C** and the different anions are shown in Figures 38-39. Upon the addition of acetate, emission enhancement could be observed with the fluorescence spectra, the peak at 445 nm is shifted to 458 nm, and a new peak

appearing at 521 nm (Figure 38a). The results of the Job plot indicates that the interaction is through hydrogen bonding, and the basicity character of acetate is associated with the deprotonation of receptor **C** when in excess [94]. Therefore, the dual emission characteristic of receptor **C** with anions interaction are attributed to hydrogen bonding and gradual deprotonation. The addition of molar equivalents of cyanide resulted in the dual emission enhancement with peaks at 453 nm and 520 nm (Figure 38b). The emission at 453 nm is likely attributed to nucleophilic addition of cyanide interaction with imine group, whereas for 520 nm, it is ascribed to deprotonation of the amine and hydroxyl group.

The fluoride addition resulted in the enhancement and a slight shift of the emission peak around 445 nm to 449 nm with a new band forming at 520 nm where enhancement is observed (Figure 38c). The addition of cyanate resulted in enhancement of emission 441 nm and the formation and enhancement of a new band at 520 nm (Figure 39a). In the same vein, the addition of hydroxide resulted in the enhancement of emission around 450nm and the formation of the enhanced band at 520 nm (Figure 39b).

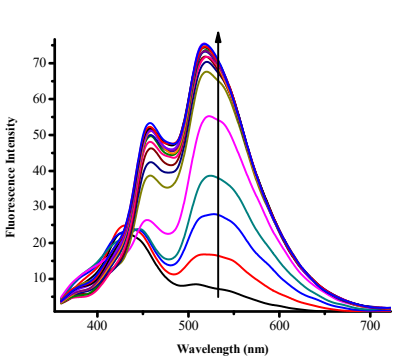

(a)

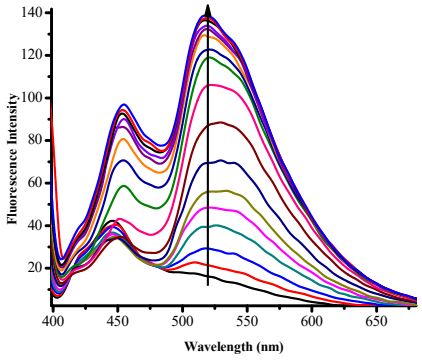

(b)

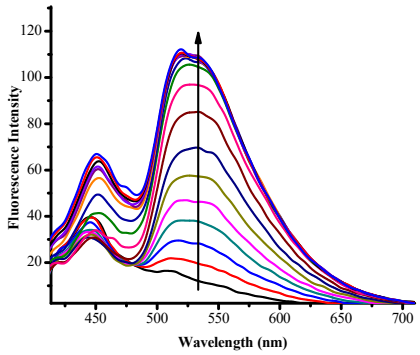

(c)

Figure 38. Fluorescence spectra of receptor **C** (1 x 10^{-5}M) in DMSO (3.0µl) in the presence of increasing amounts of 0-2.5 equiv. (a) AcO^-, (b) CN^- and (c) F^-.

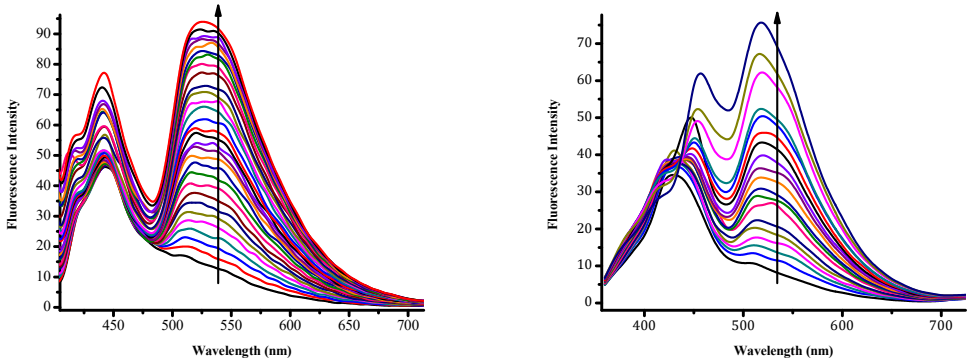

(a) (b)

Figure 39. Fluorescence spectra of receptor **C** (1 x 10^{-5}M) in DMSO (3.0µl) in the presence of increasing amounts of (a) OCN^- 0-30 equiv. and (b) OH^- 0-5 equiv.

Similarly, the cations were also investigated with the fluorescence spectroscopy. Upon the addition of Al^{3+}, receptor **C** was characterised by dual emission at 470 nm and 490 nm

(Figure 40a). The two peaks are fluorescence enhanced, and are ascribed to the tautometric forms, the keto and enol. The addition of copper, nickel and iron (Figure 40b, 40c and 41) resulted in the fluorescence quenching of the emission, and with zinc (Figure 40d), minimal change was observed with the emission. The fluorescence quenching of receptor **C** upon addition of cations is ascribed to the chelation induced quenching process, furthermore, upon the addition of mercury quenching of 441 nm due to the chelation effect. In addition, a red shift from 441 nm to 509 nm was observed with enhancement of the emission at 509 nm, and with the increasing molar addition of mercury (Figure 42), an isosbestic point could also be seen at 469 nm showing the co-existence of two species at equilibrium.

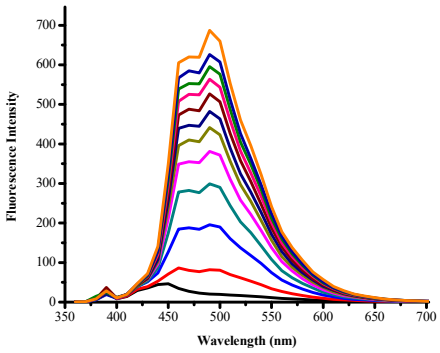

(a)

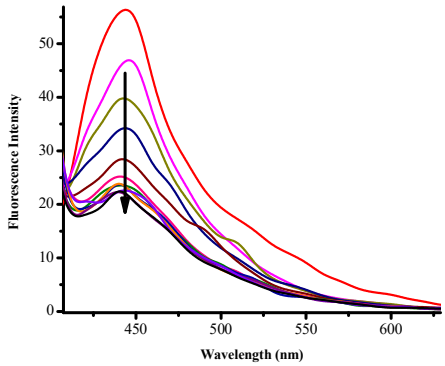

(b)

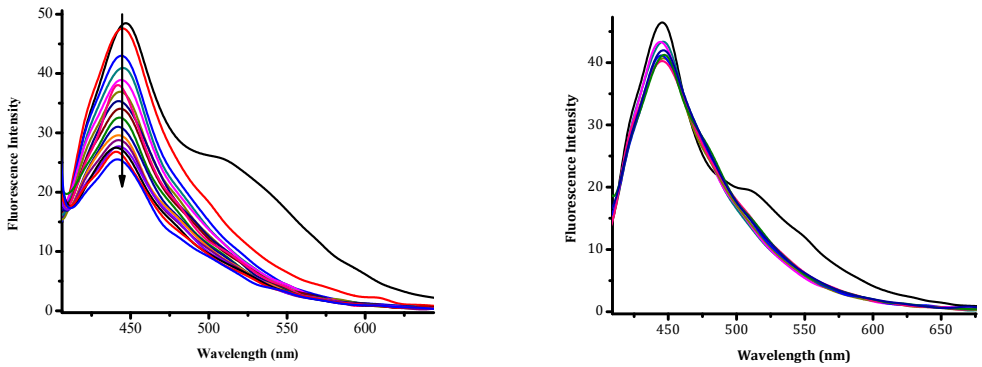

(c) (d)

Figure 40. Fluorescence spectra of receptor **C** (1 x 10^{-5}M) in DMSO (3.0µl) in the presence of increasing amounts of 0-10 equiv. (a) Al^{3+}, (b) Cu^{2+}, (c) Ni^{2+} and (d) Zn^{2+}

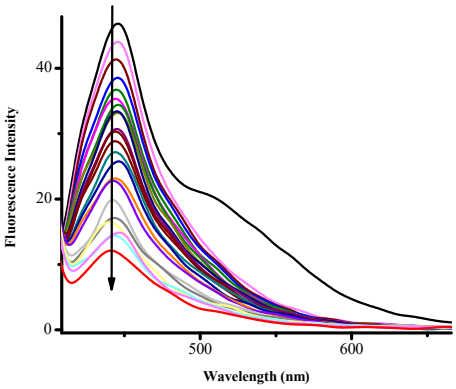

Figure 41. Fluorescence spectra of receptor **C** (1 x 10^{-5}M) in DMSO (3.0µl) in the presence of increasing amounts of 0-15 equiv. Fe^{2+}.

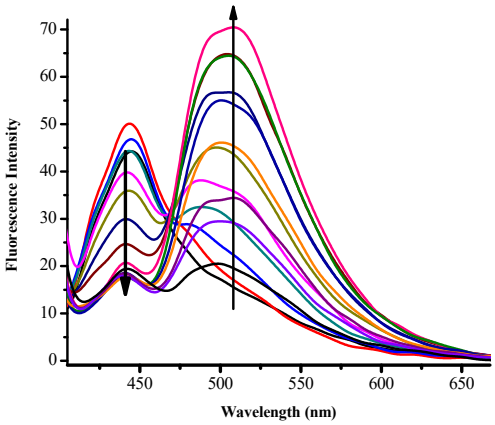

Figure 42. Fluorescence spectra of receptor **C** (1 x 10^{-5}M) in DMSO (3.0µl) in the presence of increasing amounts of 0-10 equiv. Hg^{2+}.

Chapter 5: Conclusion and recommendations

5.1 Conclusion

In this research, two dual multi-sensing and environmentally friendly receptor **A** and receptor **C** were synthesized using a cost effective single step mechanism of Schiff base in an aqueous environment. The receptors were characterized by the UV-Vis and ^{1}H NMR spectroscopic techniques. Their application to biologically important anions and toxic heavy metal ions has been studied in DMSO. The result helped to assess the receptors' ability to interact with the targeted ions. The receptor **A** displayed a strong sensing affinity towards AcO^-, F^-, CN^- and OH^- through spectroscopic techniques; however, no colorimetric sensitivity was observed. In addition, receptor **A** displayed both naked eye colorimetric sensitivity and spectrally towards cations Cu^{2+}, Fe^{2+} and Co^{2+}. The colorimetric observations were further confirmed by UV-Vis absorption spectra and fluorescence: A bathochromic shift of the absorption maxima 316 nm from 270 nm for ions and with an isosbestic point in the absorption spectra. Furthermore, fluorescence spectra of. AcO^-, F^-, CN^-, OH^-, $Cu^{2+}$and Co^{2+} displayed fluorescence enhancement, and for Fe^{2+}, fluorescence quenching.

Correspondingly, receptor **C** was able to discriminate heavy metals such as Cu^{2+}, Fe^{2+}, Ni^{2+}, Zn^{2+} and Hg^{2+} through naked eye colorimetric observations as well as spectrally. Spectrally, receptor **C** interactions with cations resulted in a variety of shifts in the spectra based on the identity of the cations in UV-Vis absorption. Fluorescence quenching was observed with most cations except for Hg^{2+} and Al^{3+} where fluorescence enhancement is perceived. Additionally, receptor **C** was also able to detect anions such as AcO^-, F^-, OCN^-, CN^-, OH^-, N_3^- and $H_2PO_4^-$, and all the anions displayed colour change from light yellow

to yellow. A bathochromic shift from 384 nm and its shoulder peak at 402 nm, as well as the peak at 337 nm disappearing forming new peaks at 432 nm and 459 nm was observed for anions (AcO^-, F^-, OCN^-, CN^- and OH^-) and fluorescence enhancement. Conclusively, the changes observed for receptor **A** and receptor **C** portray the chromogenic and fluorgenic features.

Although the interaction of receptor **A** and receptor **C** with anions is through hydrogen bonding whereas heavy metals are through coordination, to improve the proposed binding mode, ^{1}H NMR titration should be carried out in future research.

5.2 Recommendations

Although the characterization of the synthesized receptor **A** and receptor **C** were carried out by ^{1}H NMR for identification of structural elucidation, their interaction with the analytes could not be carried out as this service was outsourced. It is, therefore, recommended that to further characterize receptor **A** and receptor **C**, with Fourier transform infrared spectrometer (FT-IR) to identify the functional groups responsible for sensing ability. In addition to FT-IR, electrospray ionization mass spectrometer (ESI-MS) should also be used to aid in identifying mass/weight fragments of receptor **A** and receptor **C**. Once receptor **A** and receptor **C** are thoroughly characterized, ^{1}H NMR should be carried out for identification of [A-ion] or [C-ion] structural elucidation to improve the binding mode proposal and also, to support the UV-Vis and fluorescence data. Finally, when receptor **A** and receptor **C** are thoroughly characterized, and binding mode with the cations and anions are improved, future research could look into developing these chemosensors into testing kits.

References

1. Czarnik AW (Ohio SU, editor. Fluorescent Chemosensors for Ion and Molecule Recognition. Washington DC: American Chemical Society; 1993.

2. Wu D, Sedgwick AC, Gunnlaugsson T, Akkaya EU, Yoon J, James TD. Fluorescent chemosensors: The past, present and future. Chem Soc Rev. 2017;46(23):7105–23.

3. Pangannaya S, Kaur A, Mohan M, Raval K, Chand DK, Trivedi DR. Synthesis and spectral investigation of colorimetric receptors for the dual detection of copper and acetate ions: application in molecular logic gates. Supramol Chem [Internet]. 2017;29(8):561–74. Available from: https://www.tandfonline.com/doi/full/10.1080/10610278.2017.1298764

4. Ma L, Leng T, Wang K, Wang C, Shen Y, Zhu W. A coumarin-based fluorescent and colorimetric chemosensor for rapid detection of fluoride ion. Tetrahedron [Internet]. 2017;73(10):1306–10. Available from: http://dx.doi.org/10.1016/j.tet.2017.01.034

5. Sun B, Noller BN. Simultaneous determination of trace amounts of free cyanide and thiocyanate by a stopped- flow spectrophotometric method. 1998;32(12):3698–704.

6. Strachan S. Trace elements. Curr Anaesth Crit Care [Internet]. 2010;21(1):44–8. Available from: http://dx.doi.org/10.1016/j.cacc.2009.08.004

7. Kim H-S, Angupillai S, Son Y-A. A dual chemosensor for both Cu^{2+} and Al^{3+}: A potential Cu^{2+} and Al^{3+} switched YES logic function with an INHIBIT logic gate

and a novel solid sensor for detection and extraction of Al^{3+} ions from aqueous solution. Sensors Actuators B Chem [Internet]. 2016;222:447–58. Available from: http://linkinghub.elsevier.com/retrieve/pii/S0925400515301799

8. Que EL, Domaille DW, Chang CJ. ChemInform Abstract: Metals in Neurobiology: Probing Their Chemistry and Biology with Molecular Imaging. ChemInform [Internet]. 2008;39(33):1517–49. Available from: http://doi.wiley.com/10.1002/chin.200833267

9. Azevedo BF, Furieri LB, Pec FM, Wiggers GA, Vassallo PF, Sim MR, et al. Toxic Effects of Mercury on the Cardiovascular and Central Nervous Systems. 2012;2012.

10. Qin W, Long S, Panunzio M, Biondi S. Schiff bases: A short survey on an evergreen chemistry tool. Molecules. 2013;18(10):12264–89.

11. Al Zoubi W, Al Mohanna N. Membrane sensors based on Schiff bases as chelating ionophores - A review. Spectrochim Acta - Part A Mol Biomol Spectrosc [Internet]. 2014;132:854–70. Available from: http://dx.doi.org/10.1016/j.saa.2014.04.176

12. Kajal A, Bala S, Kamboj S, Sharma N, Saini V. Schiff Bases: A Versatile Pharmacophore. J Catal [Internet]. 2013;2013(Mic):1–14. Available from: https://www.hindawi.com/archive/2013/893512/

13. Zamani HA, Rajabzadeh G, Firouz A, Ariaii-Rad AA. Synthesis of 4-amino-6-methyl-1,2,4-triazin-5-one-3-thione and its application in construction of a highly copper(II) ion-selective electrochemical sensor. J Braz Chem Soc.

2005;16(5):1061–7.

14. Condicoes DAS, Na E, Espectrofotometrica D, Ii DEF. Quim. Nova,. 2014;37(3):564–73.

15. Mahajan RK, Kaur I, Kumar M. Silver ion-selective electrodes employing Schiff base p-tert-butyl calix[4]arene derivatives as neutral carriers. Sensors Actuators, B Chem. 2003;91(1–3):26–31.

16. Abbaspour A. Aluminium(III)-selective electrode based on a newly synthesized tetradentate Schiff base. Talanta [Internet]. 2002;58(2):397–403. Available from: http://www.sciencedirect.com/science/article/pii/S0039914002002904

17. Jeong T, Lee HK, Jeong DC, Jeon S. A lead(II)-selective PVC membrane based on a Schiff base complex of N,N′-bis(salicylidene)-2,6-pyridinediamine. Talanta. 2005;65(2 SPEC. ISS.):543–8.

18. Singh AK, Gupta VK, Gupta B. Chromium(III) selective membrane sensors based on Schiff bases as chelating ionophores. Anal Chim Acta. 2007;585(1):171–8.

19. Yu L, Wang S, Huang K, Liu Z, Gao F, Zeng W. Fluorescent probes for dual and multi analyte detection. Tetrahedron [Internet]. 2015;71(29):4679–706. Available from: http://dx.doi.org/10.1016/j.tet.2015.04.115

20. Aisen P. Iron metabolism Wessling-Resnickt and Elizabeth A Leiboldl. Proteins. 1:200–6.

21. Faroon OM, Abadin H, Keith S, Osier M, Chappell L, Diamond G, et al. Toxicological Profile for Cobalt. Agency Toxic Subst Dis Regist [Internet].

2004;(April):486. Available from: http://www.atsdr.cdc.gov/toxprofiles/tp33.pdf

22. Das KK, Das SN, Dhundasi S a. Nickel, its adverse health effects & oxidative stress. Indian J Med Res. 2008;128(4):412–25.

23. Schmidtchen FP, Berger M. Artificial Organic Host Molecules for Anions. Chem Rev [Internet]. 1997 Aug 1;97(5):1609–46. Available from: http://dx.doi.org/10.1021/cr9603845

24. Prodi L, Ciamician CG, Selmi V. Luminescent chemosensors : from molecules to nanoparticles. 2005;

25. Hulanicki A, Glab S, Ingman F. Chemical sensors definitions and classification. Pure Appl Chem. 1991;63(9):1247–50.

26. Mcdonagh C, Burke CS, Maccraith BD. Optical Chemical Sensors. 2008;353(0):400–22.

27. Suksai C, Tuntulani T. Chromogenic anion sensors. Top Curr Chem. 2005;255:163–98.

28. Martinez-Manez R, Sancenon F. Fluorogenic and Chromogenic Chemosensors and Reagents for Anions. Chem Rev [Internet]. 2003 Nov;103(11):4419–76. Available from: http://pubs.acs.org/doi/abs/10.1021/cr010421e

29. Kaur B, Kaur N, Kumar S. Colorimetric metal ion sensors – A comprehensive review of the years 2011–2016. Coord Chem Rev [Internet]. 2018;358:13–69. Available from: https://doi.org/10.1016/j.ccr.2017.12.002

30. Prodi L, Bolletta F, Montalti M, Zaccheroni N. Luminescent chemosensors for

transition metal ions. Coord Chem Rev [Internet]. 2000 [cited 2017 Apr 27];205(1):59–83. Available from: http://www.sciencedirect.com/science/article/pii/S0010854500002423

31. Wang B, Anslyn E V. Chemosensors: Principles, Strategies, and Applications. Chemosensors: Principles, Strategies, and Applications. 2011.

32. Li Y, Xie W, Fang G. Fluorescence detection techniques for protein kinase assay. 2008;2049–57.

33. Matsumoto A. Topics in Current Chemistry Editorial Board : [Internet]. Top Curr Chem. 2005. 263–305 p. Available from: https://www.researchgate.net/profile/Dario_Braga/publication/225896407_Intra-Solid_and_Inter-Solid_Reactions_of_Molecular_Crystals_a_Green_Route_to_Crystal_Engineering/links/0046352d0e623d374d000000.pdf#page=242

34. Okudan A, Erdemir S, Kocyigit O. “Naked-eye” detection of fluoride and acetate anions by using simple and efficient urea and thiourea based colorimetric sensors. J Mol Struct. 2013;

35. Bangs LB. New developments in particle-based immunoassays: introduction. 1996;68(10):1873–9.

36. Blake DA, McLean N V. A colorimetric assay for the measurement of d-glucose consumption by cultured cells. Anal Biochem. 1989;177(1):156–60.

37. Kang J, Jo JH, In S. Carboxylate anion selective receptor with glycoluril molecular scaffold. Tetrahedron Lett. 2004;45(27):5225–8.

38. Lhota P, Stibor I, Lang K. Calix [4] arene-porphyrin Conjugates as Versatile Molecular Receptors for. 2002;(c):7343–6.

39. Burns DH, Calderon-Kawasaki K, Kularatne S. Buried solvent determines both anion-binding selectivity and binding stoichiometry with hydrogen-bonding receptors. J Org Chem. 2005;70(7):2803–7.

40. Kato R, Nishizawa S, Hayashita T, Teramae N. Tetrahed.Lett.2001.5053-5056-ThioureaSensors. 2001;42:1–4. Available from: http://www.sciencedirect.com/science?_ob=MImg&_imagekey=B6THS-43DF4G2-11-1&_cdi=5290&_user=496085&_pii=S0040403901009169&_origin=gateway&_coverDate=07%2F23%2F2001&_sk=999579969&view=c&wchp=dGLbVlz-zSkzV&md5=b286ece455e85db7982c5bbbc0c7690f&ie=/sdarticle.p

41. Black CB, Andrioletti B, Try AC, Ruiperez C, Sessler JL. Dipyrrolylquinoxalines: Efficient sensors for fluoride anion in organic solution [12]. J Am Chem Soc [Internet]. 1999;121(44):10438–9. Available from: https://pubs.acs.org/doi/pdf/10.1021/ja992579a

42. Goswami S, Das AK, Sen D, Aich K, Fun HK, Quah CK. A simple naphthalene-based colorimetric sensor selective for acetate. Tetrahedron Lett [Internet]. 2012;53(36):4819–23. Available from: http://dx.doi.org/10.1016/j.tetlet.2012.06.104

43. Vilar R, editor. Recognition of Anions [Internet]. Berlin, Heidelberg: Springer Berlin Heidelberg; 2008. 262 p. (Structure and Bonding; vol. 129). Available

from: http://link.springer.com/10.1007/978-3-540-79092-1

44. Raymo FM. Digital processing and communication with molecular switches. Adv Mater. 2002;14(6):401–14.

45. Mondal J, Manna AK, Patra GK. Highly selective hydrazone based reversible colorimetric chemosensors for expeditious detection of CN^- in aqueous media. Inorganica Chim Acta [Internet]. 2018;474:22–9. Available from: https://doi.org/10.1016/j.ica.2018.01.013

46. ATSDR. Toxicological Profile for vinyl acetate. Oxid Med Cell Longev [Internet]. 2013;2013(205):24. Available from: http://dx.doi.org/10.1155/2013/286524

47. Goswami S, Das MK, Manna A. Pterin-based highly selective, ratiometric, and sensitive “naked-eye” sensor for acetate. Tetrahedron Lett. 2014;55(16):2707–10.

48. Kandelbauer A. Cyanate Esters [Internet]. Handbook of Thermoset Plastics. Elsevier Inc.; 2013. 425–457 p. Available from: http://dx.doi.org/10.1016/B978-1-4557-3107-7.00011-7

49. El-Gamal D, Rao SP, Holzer M, Hallstrom S, Haybaeck J, Gauster M, et al. The urea decomposition product cyanate promotes endothelial dysfunction. Kidney Int. 2014;86(5):923–31.

50. Foundation C. Cyanide compounds in biology. Evered D, Harnett S, editors. Chichester, UK.: John wiley & sons Chichester; 1988. 270 p.

51. Abraham K, Buhrke T, Lampen A. Bioavailability of cyanide after consumption

of a single meal of foods containing high levels of cyanogenic glycosides : a crossover study in humans. Arch Toxicol [Internet]. 2016;559–74. Available from: http://dx.doi.org/10.1007/s00204-015-1479-8

52. Sun P, Borowitz JL, Kanthasamy AG, Gunasekar PG, E G. Antagonism of cyanide toxicity by isosorbide dinitrate : possible role of nitric oxide. 1995;104:105–11.

53. Conn EE. Cyanogenesis, The production of hydrogen cyanide, by plants. Eff Poisonous Plants Livest [Internet]. 1978 Jan 1 [cited 2018 Aug 21];301–10. Available from: https://www.sciencedirect.com/science/article/pii/B9780124032507500352

54. Zheng X, Zhu W, Ai H, Huang Y, Lu Z. A rapid response colorimetric and ratiometric fluorescent sensor for detecting fluoride ion, and its application in real sample analysis. Tetrahedron Lett [Internet]. 2016;57(52):5846–9. Available from: http://dx.doi.org/10.1016/j.tetlet.2016.11.032

55. Chen X, Leng T, Wang C, Shen Y, Zhu W. A highly selective naked-eye and fluorescent probe for fluoride ion based on 1,8-naphalimide and benzothizazole. Dye Pigment [Internet]. 2017;141:299–305. Available from: http://linkinghub.elsevier.com/retrieve/pii/S0143720816314103

56. Fu L, Wang FF, Gao T, Huang R, He H, Jiang FL, et al. Highly efficient fluorescent BODIPY dyes for reaction-based sensing of fluoride ions. Sensors Actuators, B Chem. 2015;216:558–62.

57. Udhayakumari D, Velmathi S. Naphthalene thiourea derivative based colorimetric

and fluorescent dual chemosensor for F^- and Cu^{2+} /Hg^{2+} ions. Supramol Chem [Internet]. 2015;27(7–8):539–44. Available from: http://www.tandfonline.com/doi/full/10.1080/10610278.2015.1025784

58. Li D, Zhong Z, Zheng G, Tian Z. A naphthalene benzimidazole-based chemosensor for the colorimetric and on-off fluorescent detection of fluoride ion. Spectrochim Acta Part A Mol Biomol Spectrosc [Internet]. 2017;185:173–8. Available from: http://linkinghub.elsevier.com/retrieve/pii/S1386142517304298

59. Sivamani J, Siva A. Self-assembly, "turn-on" fluorescent detection of fluoride ion using uracil based azo derivatives and their application in imaging of living cells. Sensors Actuators, B Chem [Internet]. 2017;242:423–33. Available from: http://dx.doi.org/10.1016/j.snb.2016.11.069

60. Kumar V, Kaushik MP, Srivastava AK, Pratap A, Thiruvenkatam V, Row TNG. Analytica Chimica Acta Thiourea based novel chromogenic sensor for selective detection of fluoride and cyanide anions in organic and aqueous media. 2010;663:77–84.

61. Shan R ran, Yan L guo, Yang Y ming, Yang K, Yu S jun, Yu H qin, et al. Highly efficient removal of three red dyes by adsorption onto Mg-Al-layered double hydroxide. J Ind Eng Chem [Internet]. 2015;21:561–8. Available from: http://dx.doi.org/10.1016/j.jiec.2014.03.019

62. Gu Z, Atherton JJ, Xu ZP. Hierarchical layered double hydroxide nanocomposites: structure, synthesis and applications. Chem Commun. 2015;15(51):3024–36.

63. Wang X, Zhou W, Wang C, Chen Z. In situ immobilization of layered double hydroxides onto cotton fiber for solid phase extraction of fluoroquinolone drugs. Talanta [Internet]. 2018;186(January):545–53. Available from: https://doi.org/10.1016/j.talanta.2018.04.100

64. Choy JH, Choi SJ, Oh JM, Park T. Clay minerals and layered double hydroxides for novel biological applications. Appl Clay Sci. 2007;36(1–3):122–32.

65. Velmathi S, Reena V. Pyrrole Based Schiff Bases as Colorimetric and Fluorescent Chemosensors for Fluoride and Hydroxide Anions. 2012;155–62.

66. Sivaraman G, Iniya M, Anand T, Kotla NG, Sunnapu O, Singaravadivel S, et al. Chemically diverse small molecule fluorescent chemosensors for copper ion. Coord Chem Rev [Internet]. 2018;357:50–104. Available from: https://doi.org/10.1016/j.ccr.2017.11.020

67. Manna AK, Mondal J, Chandra R, Rout K, Patra GK. A thio-urea based chromogenic and fluorogenic chemosensor for expeditious detection of Cu^{2+}, $Hg^{2+}$and Ag^{+}ions in aqueous medium. J Photochem Photobiol A Chem [Internet]. 2018;356:477–88. Available from: http://dx.doi.org/10.1016/j.jphotochem.2018.01.017

68. Na YJ, Choi YW, You GR, Kim C. A novel selective colorimetric chemosensor for cobalt ions in a near perfect aqueous solution. Sensors Actuators, B Chem [Internet]. 2016;223:234–40. Available from: http://dx.doi.org/10.1016/j.snb.2015.09.098

69. Leyssens L, Vinck B, Van Der Straeten C, Wuyts F, Maes L. Cobalt toxicity in

humans—A review of the potential sources and systemic health effects. Toxicology [Internet]. 2017;387(March):43–56. Available from: http://dx.doi.org/10.1016/j.tox.2017.05.015

70. Opinion S. Scientific opinion on safety and efficacy of cobalt compounds (E3) as feed additives for all animal species: cobaltous acetate tetrahydrate, basic cobaltous carbonate monohydrate and cobaltous sulphate heptahydrate, based on a dossier submitted by TREACE EEIG. EFSA J [Internet]. 2012;10(7):2791. Available from: http://www.efsa.europa.eu/en/efsajournal/doc/2791.pdf

71. Ou D, Zhang L, Yanfen H, Xiaoding L, Qin J, Li Z. A new disubstituted polyacetylene bearing 6-Benzylaminopurine moieties : Postfunctional synthetic strategy and sensitive chemosensor towards Copper and Cobalt ions. Macromol Rapid Commun. 2013;13:759–66.

72. Liu Z, Wang W, Xu H, Sheng L, Chen S, Huang D, et al. A “naked eye” and ratiometric chemosensor for cobalt(II) based on coumarin platform in aqueous solution. Inorg Chem Commun [Internet]. 2015;62:19–23. Available from: http://dx.doi.org/10.1016/j.inoche.2015.10.017

73. Hens A, Maity A, Rajak KK. N, N coordinating schiff base ligand acting as a fluorescence sensor for zinc(II) and colorimetric sensor for copper(II), and zinc(II) in mixed aqueous media. Inorganica Chim Acta [Internet]. 2014;423(PA):408–20. Available from: http://dx.doi.org/10.1016/j.ica.2014.08.024

74. Qin J, Yang Z. Design of a novel coumarin-based multifunctional fl uorescent

probe for Zn^{2+} / Cu^{2+} / S^{2-} in aqueous solution. Mater Sci Eng C [Internet]. 2015;57:265–71. Available from: http://dx.doi.org/10.1016/j.msec.2015.07.064

75. Aksuner N, Henden E, Yilmaz I, Cukurovali A. A highly sensitive and selective fluorescent sensor for the determination of copper(II) based on a schiff base. Dye Pigment. 2009;83(2):211–7.

76. Kundu A, Hariharan PS, Prabakaran K, Anthony SP. Synthesis of new colori/fluorimetric chemosensor for selective sensing of biologically important Fe^{3+}, Cu^{2+} and Zn^{2+} metal ions. Spectrochim Acta A Mol Biomol Spectrosc [Internet]. 2015;151:426–31. Available from: http://www.sciencedirect.com/science/article/pii/S1386142515300263

77. Hammud HH, El Shazly S, Sonji G, Sonji N, Bouhadir KH. Thiophene aldehyde-diamino uracil Schiff base: A novel fluorescent probe for detection and quantification of cupric, silver and ferric ions. Spectrochim Acta - Part A Mol Biomol Spectrosc [Internet]. 2015;150:94–103. Available from: http://dx.doi.org/10.1016/j.saa.2015.05.038

78. Uahengo V, Zhang Y, Xiong B, Zhao P, Cai P, Rhyman L, et al. A Fluoro-Chromogenic Sensor Based on Organic Molecular Framework for Cu^{2+} and F^{-} in Aqueous Soluble DMSO. Journal of Fluorescence. 2017.

79. Sigel A, Sigel H. Metal Ions in Biological Systems. 2004. 530 p.

80. McLellan SA, Walsh TS. Oxygen delivery and haemoglobin. Contin Educ Anaesthesia, Crit Care Pain. 2004;4(4):123–6.

81. Murphy JF, Newcombe RG, O'Riordan J, Coles EC, Pearson JF. Relation of

haemoglobin levels in first and second trimesters to outcome of pregnancy. Lancet [Internet]. 1986 May 3 [cited 2018 Aug 21];327(8488):992–5. Available from: https://www.sciencedirect.com/science/article/pii/S0140673686912699

82. Rana D, M Rana A, Sahoo SK. Cation Sensing of Pyridoxal Derived Sensors Towards Fe (II) Ion in Pure Aqueous Solution. Chem Sci J. 2018;08(04):8–12.

83. Clarkson TW, Magos L, Myers GJ. The Toxicology of Mercury — Current Exposures and Clinical Manifestations. N Engl J Med [Internet]. 2003;349(18):1731–7. Available from: http://www.nejm.org/doi/abs/10.1056/NEJMra022471

84. Tchounwou PB, Ayensu WK, Ninashvili N, Sutton D. Environmental exposure to mercury and its toxicopathologic implications for public health. Environ Toxicol. 2003;18(3):149–75.

85. Clarkson TW, Magos L. The Toxicology of Mercury and Its Chemical Compounds. Crit Rev Toxicol [Internet]. 2006 Jan 1;36(8):609–62. Available from: https://doi.org/10.1080/10408440600845619

86. Kou S, Nam S, Shumi W, Lee MH, Bae SW, Du J, et al. Microfluidic Detection of Multiple Heavy Metal Ions Using Fluorescent Chemosensors. 2009;30(5):1173–6.

87. Jonaghani MZ, Zali-boeini H. Spectrochimica Acta Part A : Molecular and Biomolecular Spectroscopy Highly selective fl uorescent and colorimetric chemosensor for detection of Hg^{2+} ion in aqueous media. Spectrochim Acta Part A Mol Biomol Spectrosc [Internet]. 2017;178:66–70. Available from:

http://dx.doi.org/10.1016/j.saa.2017.01.065

88. Coogan TP, Latta DM, Snow ET, Costa M, Lawrence A. Toxicity and Carcinogenicity of Nickel Compounds. CRC Crit Rev Toxicol [Internet]. 1989 Jan 26 [cited 2018 Sep 22];19(4):341–84. Available from: http://www.tandfonline.com/doi/full/10.3109/10408448909029327

89. Jiang J, Gou C, Luo J, Yi C, Liu X. A novel highly selective colorimetric sensor for Ni (II) ion using coumarin derivatives. INOCHE [Internet]. 2012;15:12–5. Available from: http://dx.doi.org/10.1016/j.inoche.2011.09.027

90. Choi YW, Park GJ, Na YJ, Jo HY, Lee SA, You GR, et al. A single schiff base molecule for recognizing multiple metal ions: A fluorescence sensor for Zn(II) and Al(III) and colorimetric sensor for Fe(II) and Fe(III). Sensors Actuators, B Chem [Internet]. 2014;194:343–52. Available from: http://dx.doi.org/10.1016/j.snb.2013.12.114

91. Hu J, Li J, Qi J, Sun Y. Sensors and Actuators B : Chemical Acylhydrazone based fluorescent chemosensor for zinc in aqueous solution with high selectivity and sensitivity. Sensors Actuators B Chem [Internet]. 2015;208:581–7. Available from: http://dx.doi.org/10.1016/j.snb.2014.11.066

92. Sutariya PG, Modi NR, Pandya A, Joshi BK, Joshi K V., Menon SK. An ICT based “turn on/off” quinoline armed calix[4]arene fluoroionophore: Its sensing efficiency towards fluoride from waste water and Zn^{2+} from blood serum. Analyst. 2012;137(23):5491–4.

93. Upadhyay KK, Mishra RK, Kumar V, Chowdhury PKR. A coumarin based ICT

probe for fluoride in aqueous medium with its real application. Talanta [Internet]. 2010;82(1):312–8. Available from: http://dx.doi.org/10.1016/j.talanta.2010.04.041

94. Kuzu B, Tan M, Ekmekci Z, Menges N. A novel structure for ESIPT emission: Experimental and theoretical investigations. J Photochem Photobiol A Chem [Internet]. 2019;381(October 2018):111874. Available from: https://doi.org/10.1016/j.jphotochem.2019.111874

Appendices

Appendix 1: ^{1}H NMR spectrum of receptors

Appendix 1.1. ^{1}H NMR spectral of receptor **A** in DMSO-d_6

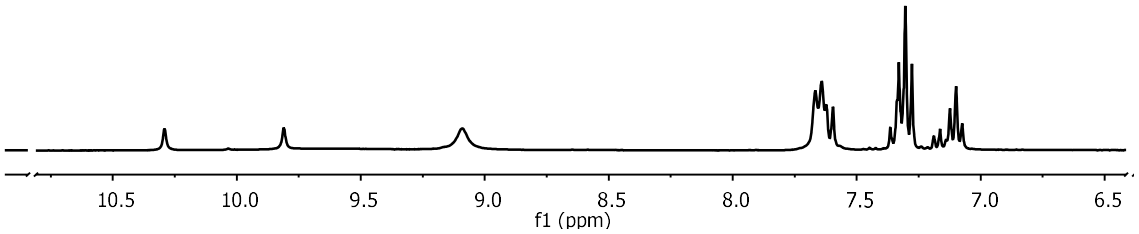

Appendix 1.2. ^{1}H NMR spectral of receptor **C** in DMSO-d_6

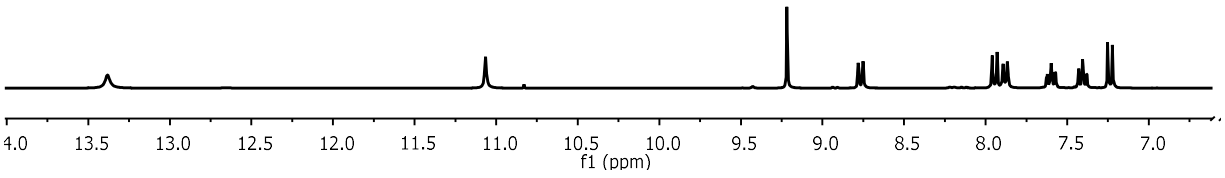

Appendix 2: Ethical clearance certificate

UNAM
UNIVERSITY OF NAMIBIA

ETHICAL CLEARANCE CERTIFICATE

Ethical Clearance Reference Number: FOS /300/2017 **Date: 10 October, 2017**

This Ethical Clearance Certificate is issued by the University of Namibia Research Ethics Committee (UREC) in accordance with the University of Namibia's Research Ethics Policy and Guidelines. Ethical approval is given in respect of undertakings contained in the Research Project outlined below. This Certificate is issued on the recommendations of the ethical evaluation done by the Faculty/Centre/Campus Research & Publications Committee sitting with the Postgraduate Studies Committee.

Title of Project: The Synthesis And Characterization Of Chemical Sensors And Their Application To Anions And Heavy Metal Ions Sensing

Researcher: Martha Niishiye Amputu

Student Number: 200613154

Faculty: Faculty of Science

Supervisors: Dr. Veikko Uahengo

Take note of the following:

(a) Any significant changes in the conditions or undertakings outlined in the approved Proposal must be communicated to the UREC. An application to make amendments may be necessary.

(b) Any breaches of ethical undertakings or practices that have an impact on ethical conduct of the research must be reported to the UREC.

(c) The Principal Researcher must report issues of ethical compliance to the UREC (through the Chairperson of the Faculty/Centre/Campus Research & Publications Committee) at the end of the Project or as may be requested by UREC.

(d) The UREC retains the right to:

(i) Withdraw or amend this Ethical Clearance if any unethical practices (as outlined in the Research Ethics Policy) have been detected or suspected,

(ii) Request for an ethical compliance report at any point during the course of the research.

UREC wishes you the best in your research.

Prof. P. Odonkor: UREC Chairperson

Ms. P. Claassen: UREC Secretary

Appendix 3: Supplementary information

Absorption spectra of chemosensor A with different anions

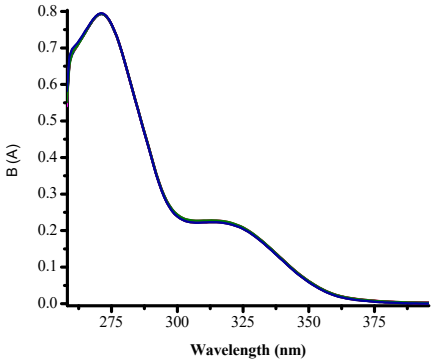

(a) Br^-

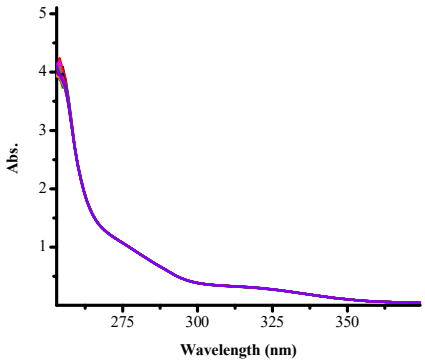

(b) Cl^-

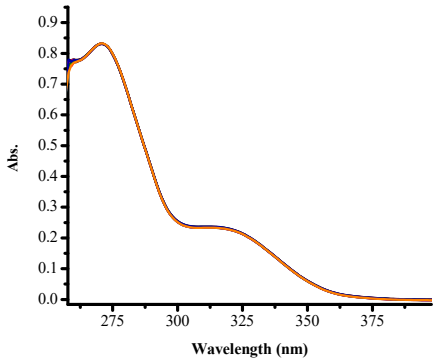

(c) ClO_4^-

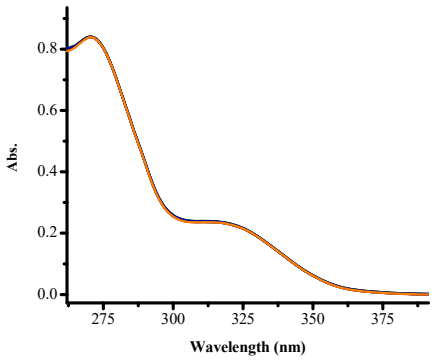

(d) HSO_4^-

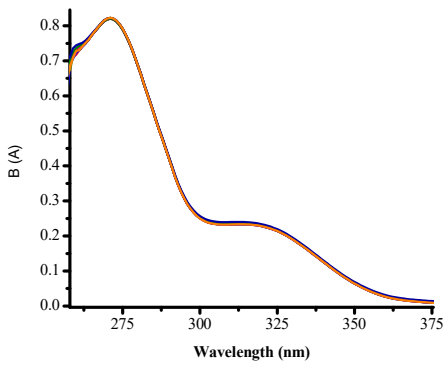

(e) I^-

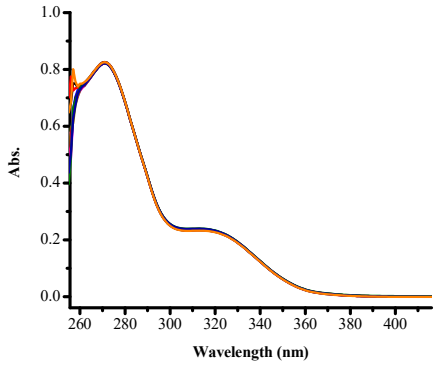

(f) N_3^-

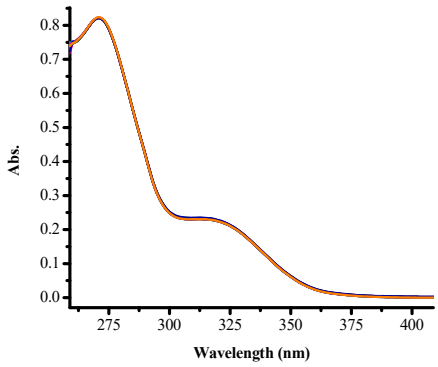

(g) NO_3^-

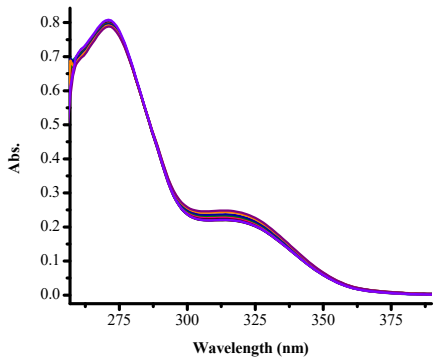

(h) $H_2PO_4^-$

Figure S1: The absorption titration spectra of receptor **A** ($1x10^{-5}$ M) in DMSO with 3 equiv. Of (a) Br^-, (b) Cl^-, (c) ClO_4^-, (d) HSO_4^-, (e) I^-, (f) N_3^-, (g) NO_3^- and (h) $H_2PO_4^-$ at ambient temperature.

UV-Vis titration of chemosensor A with cations

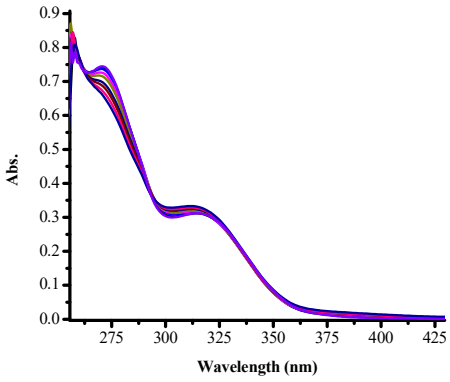

(a)Ag^{+}

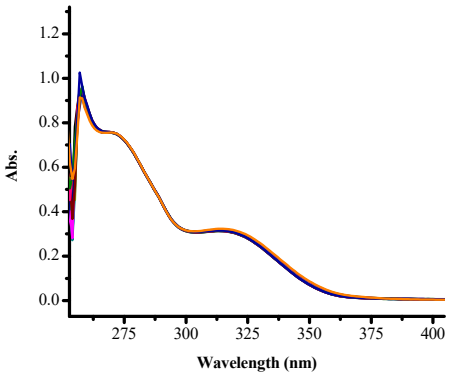

(b) Al^{3+}

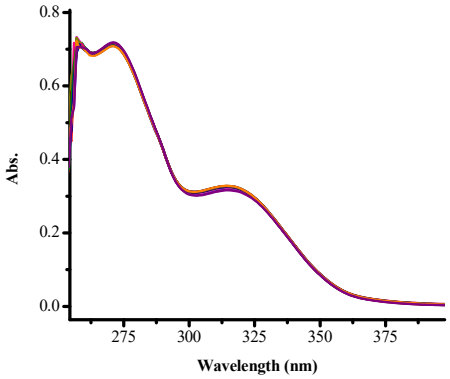

(c) Cd^{2+}

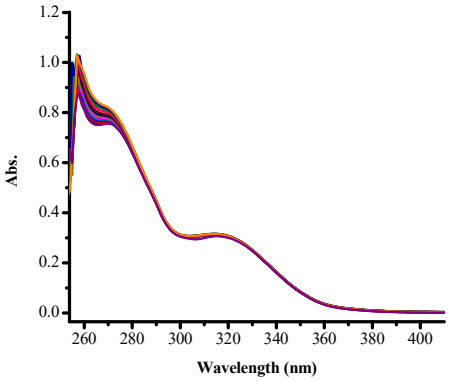

(d) Cr^{3+}

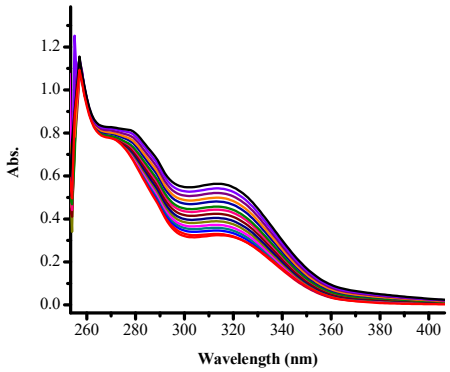

(e) Fe^{3+}

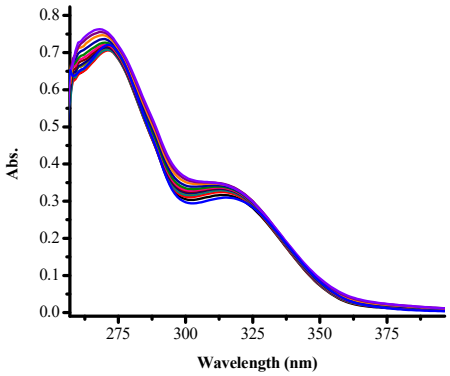

(f) Hg^{2+}

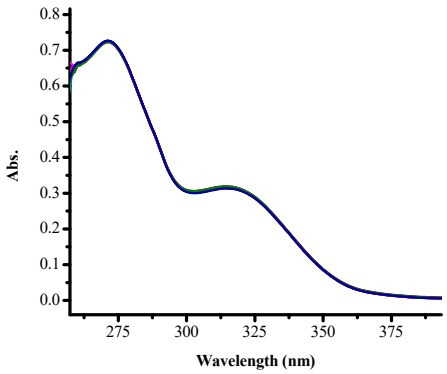

(g) Mg^{2+}

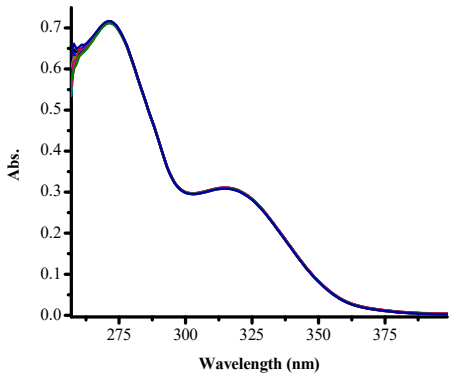

(h) Mn^{2+}

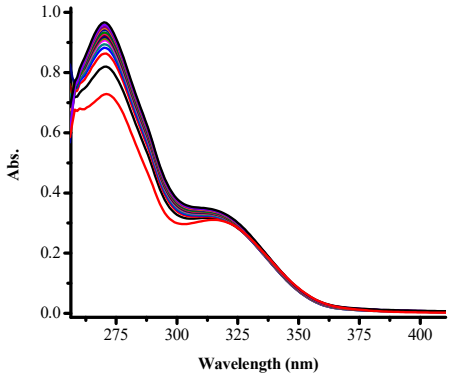

(i) Ni^{2+}

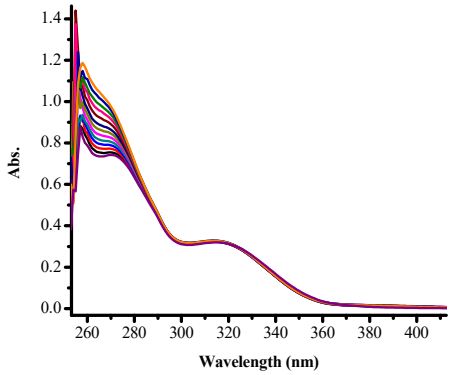

(j) Pb^{2+}

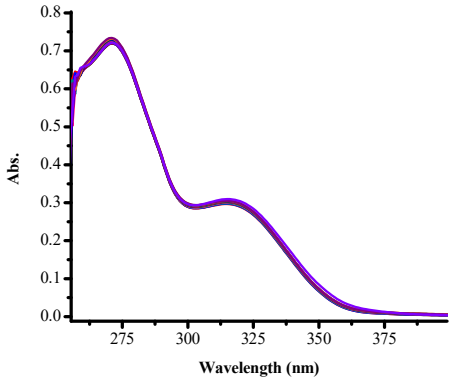

(k) Sn^{2+}

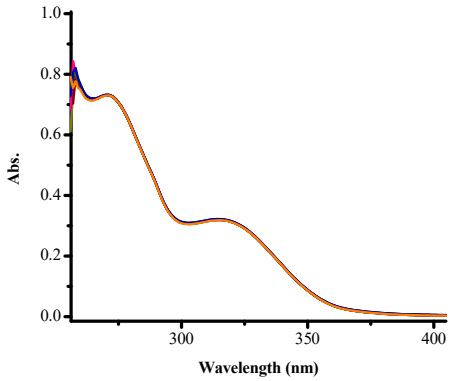

(l) Sr^{2+}

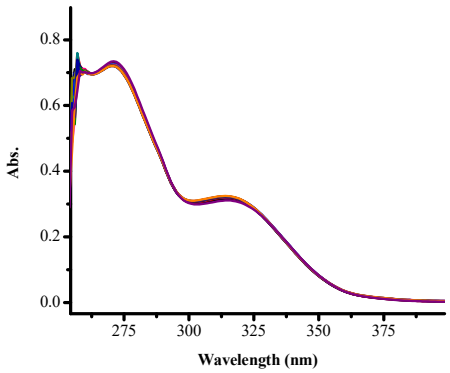

(m) Zn^{2+}

Figure S2: The absorption titration spectra of receptor **A** ($1x10^{-5}$ M) in DMSO with 3 equiv. Of (a) Ag^{+}, (b) Al^{3+}, (c) Cd^{2+}, (d) Cr^{3+}, (e) Fe^{3+}, (f) Hg^{2+}, (g) Mg^{2}, (h) Mn^{2+}, (i) Ni^{2+}, (j) Pb^{2+}, (k) Sn^{2+} , (l) Sr^{2+} and (m) Zn^{2+} at ambient temperature.

UV-Vis titration of receptor C with anions

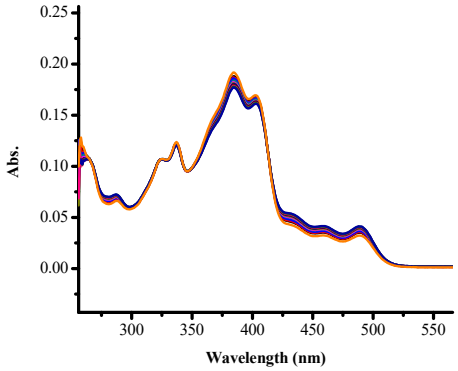

(a) Br^-

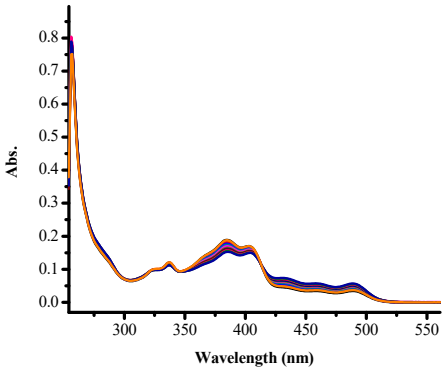

(b) Cl^-

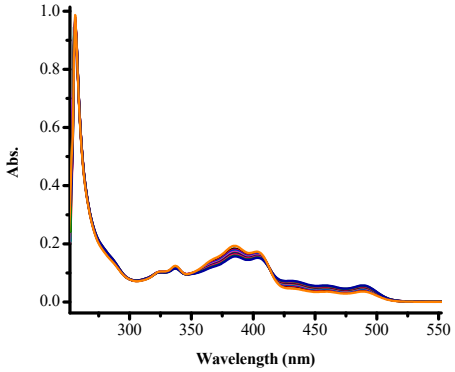

(c) ClO_4^-

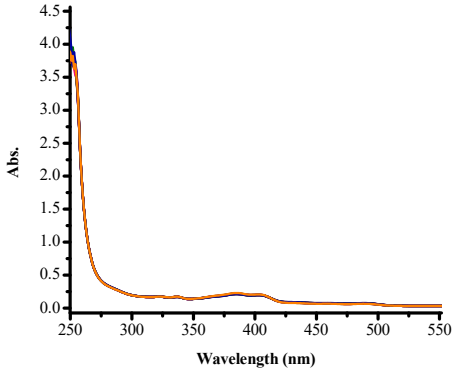

(d) HSO_4^-

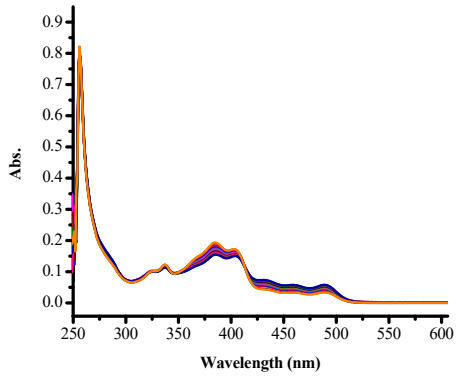

(e) I^-

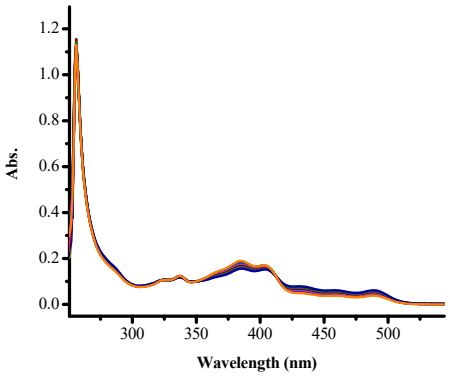

(f) NO_3^-

Figure S3. The absorption titration spectra of receptor **C** ($1x10^{-5}$ M) in DMSO with 3 equiv. Of (a) Br^-, (b) Cl^-, (c) ClO_4^-, (d) HSO_4^-, (e) I^- and (f) NO_3^- at ambient temperature.

UV-Vis titration of receptor C with cations

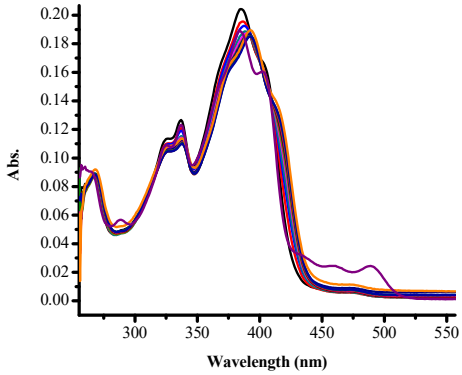

(a) Ag^+

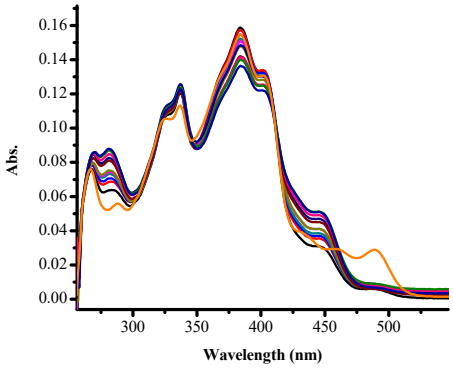

(b) Cd^{2+}

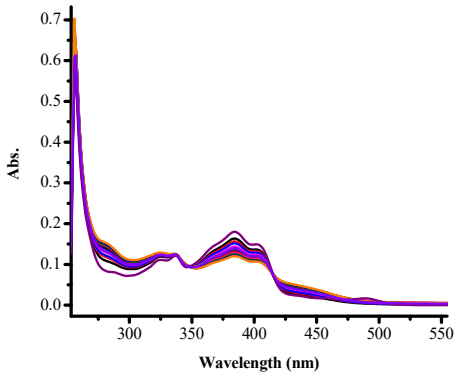

(c) Co^{2+}

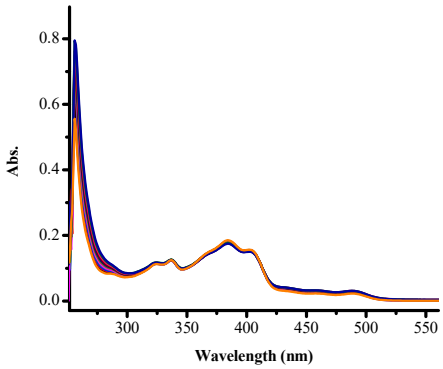

(d) Cr^{3+}

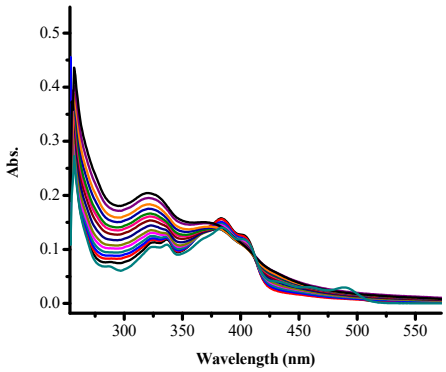

(e) Fe^{3+}

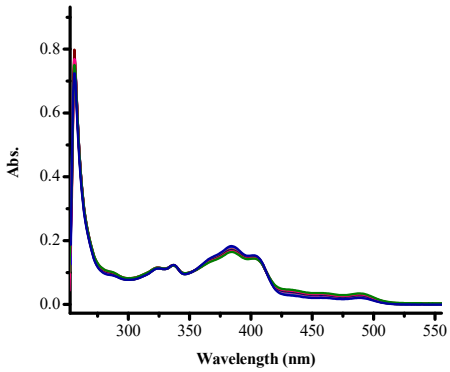

(f) Mg^{2+}

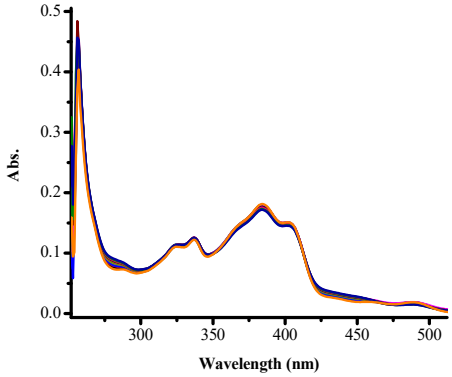

(g) Mn^{2+}

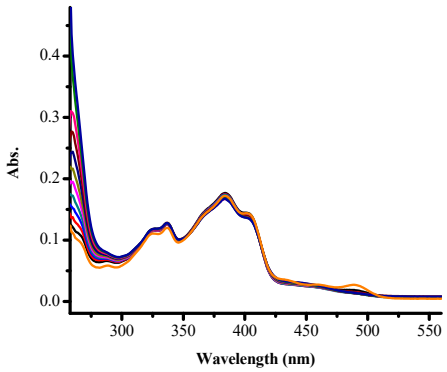

(h) Pb^{2+}

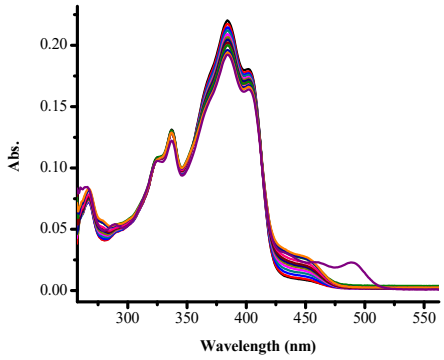

(i)Sn^{2+}

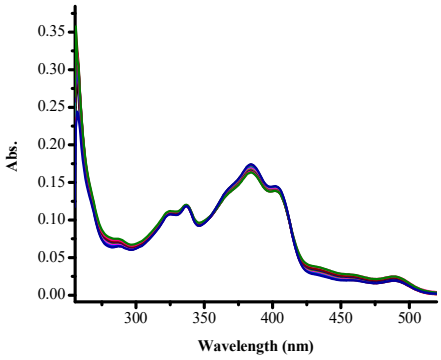

(j) Sr^{2+}

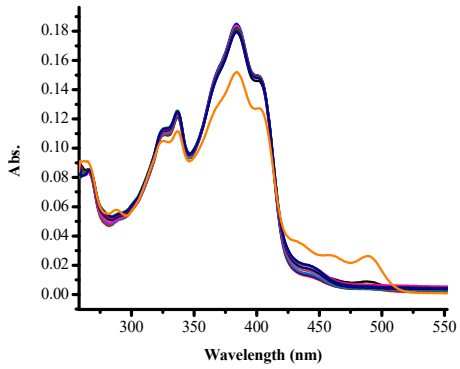

(k) Al^{3+}

Figure S4. The absorption titration spectra of receptor **C** ($1x10^{-5}$ M) in DMSO with 3 equiv. Of (a) Ag^{+}, (b) Cd^{2+}, (c) Co^{2+}, (d) Cr^{3+}, (e) Fe^{3+}, (f) Mg^{2+}, (g) Mn^{2+}, (h) Pb^{2+}, (i) Sn^{2+} (j) Sr^{2+} and (k) Al^{3+} at ambient temperature.